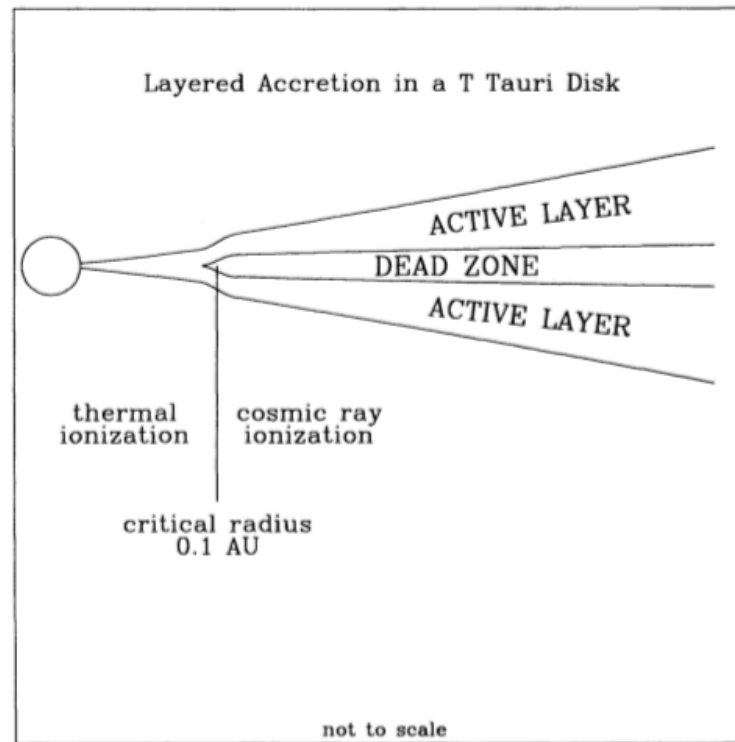


Class 15 – Mar 12th, 2020

Highly ionized disks -> MRI
Weakly ionized disks -> ?



Some MHD “rules-of-thumb”

Field lines do not want to be bent
(magnetic tension; resists stretching)



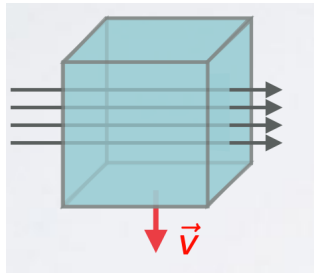
Field lines do not want to be close to each other
(magnetic pressure; resists compression)



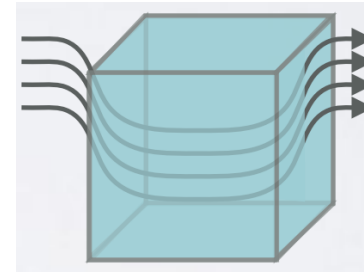
Some MHD “rules-of-thumb”

Behavior depends on the field strength

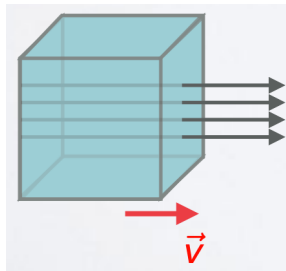
Weak field: $P_{mag} \ll P_{th}$



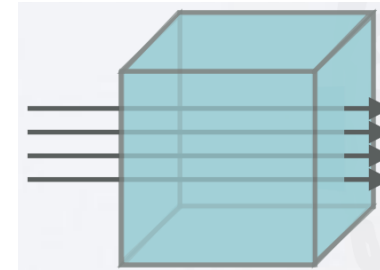
Magnetic field forced along gas flow
(passively advected)



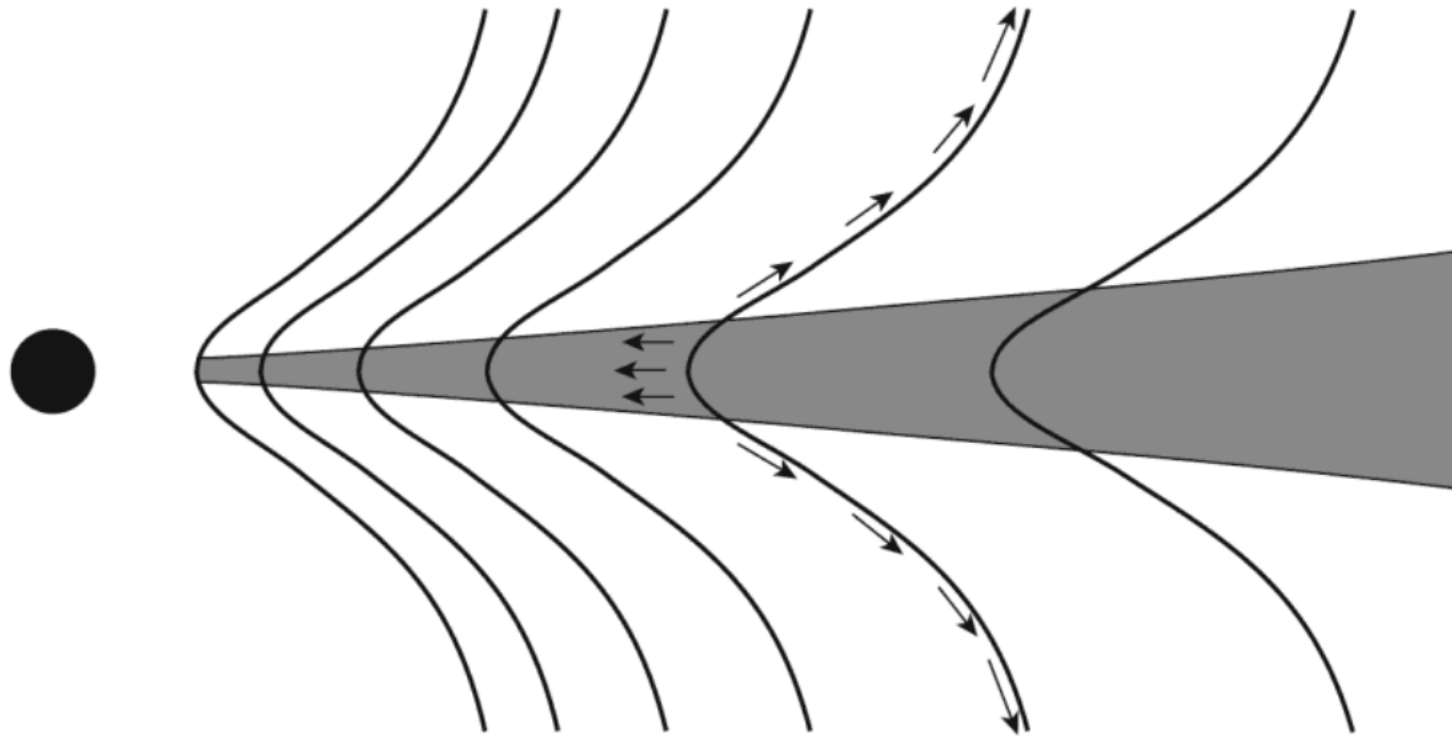
Strong field: $P_{mag} \gg P_{th}$



Gas can only move along magnetic field lines



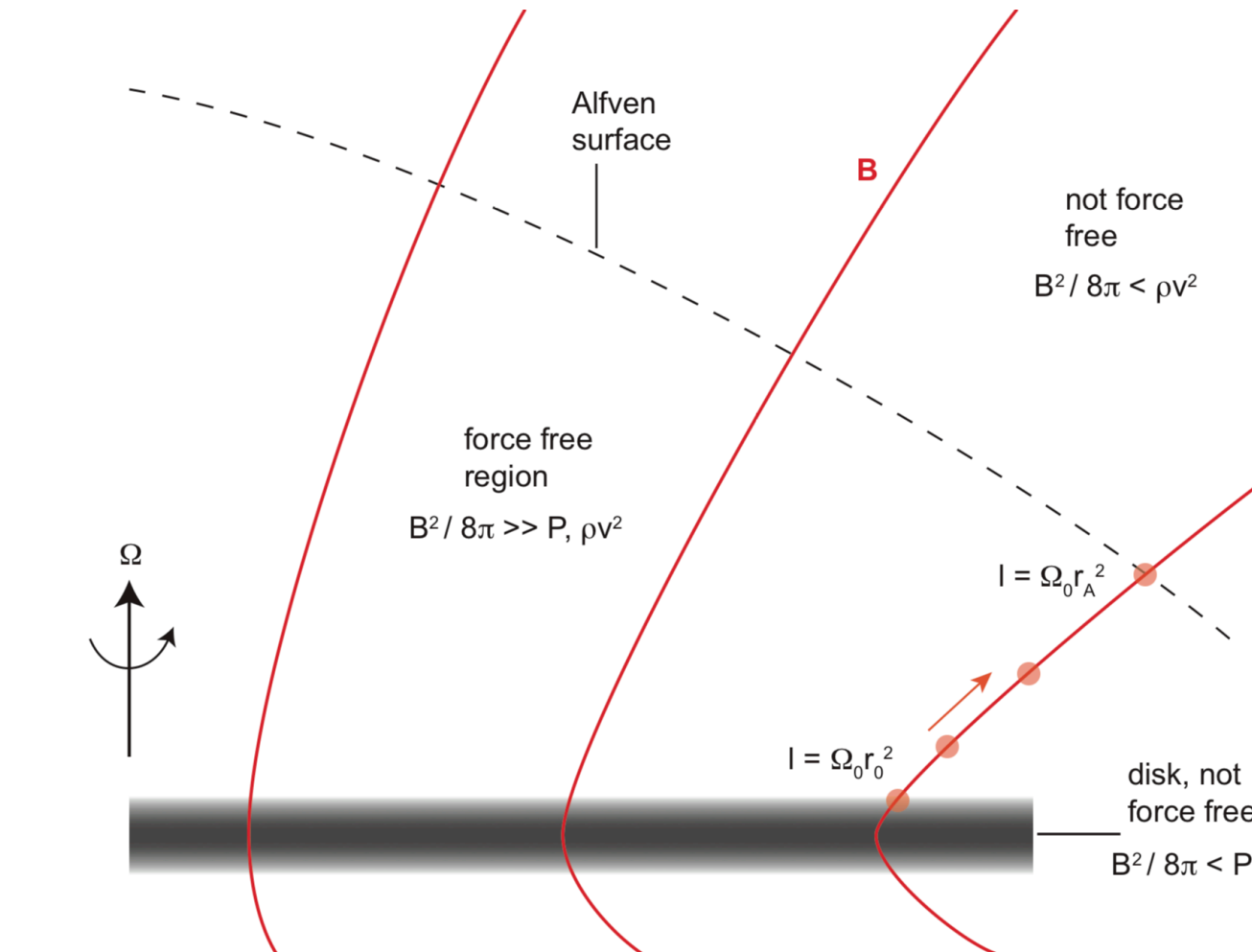
Disk winds

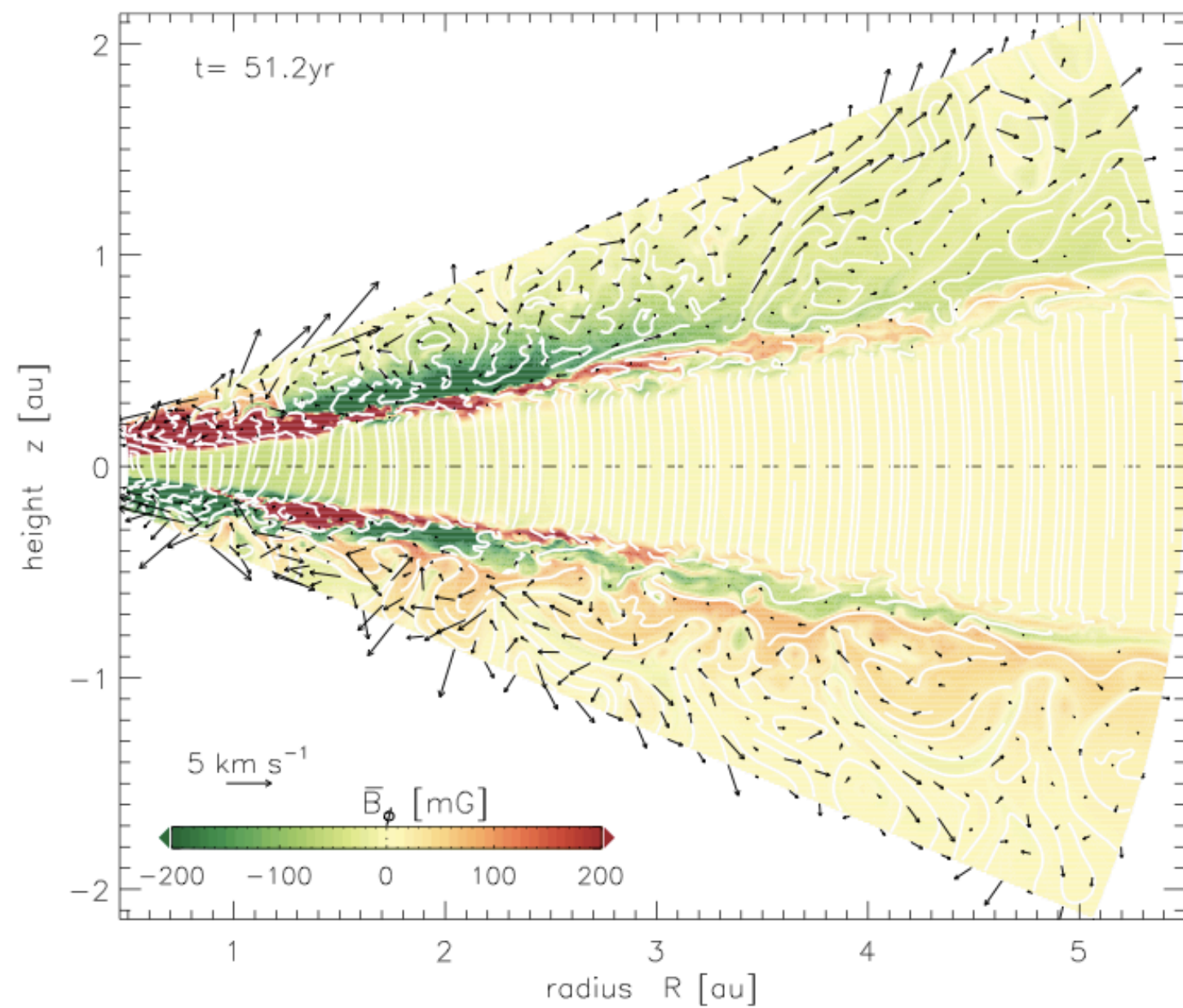


Magnetic torques remove angular momentum from gas

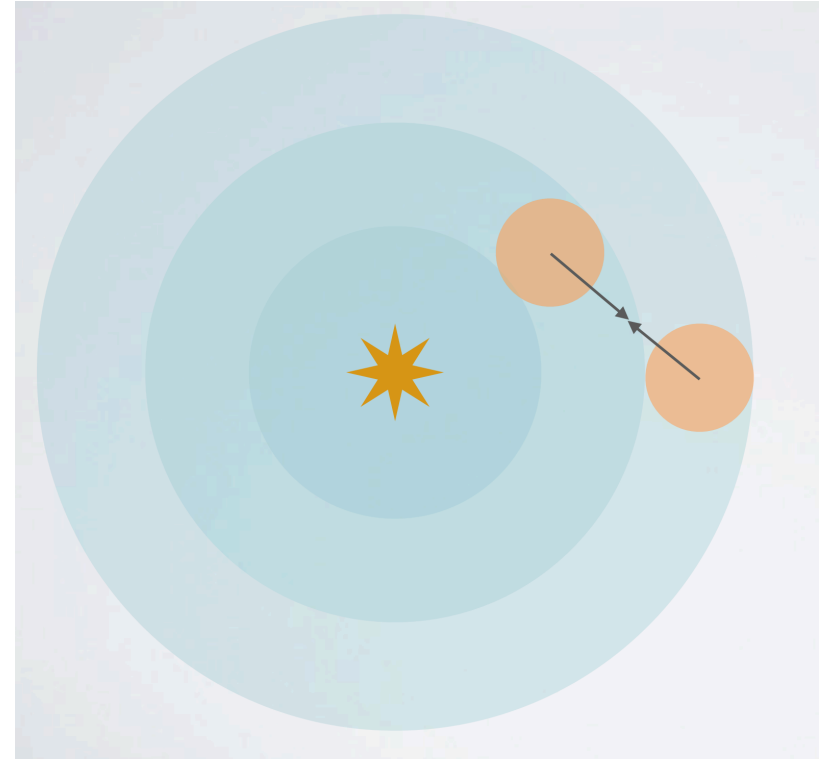
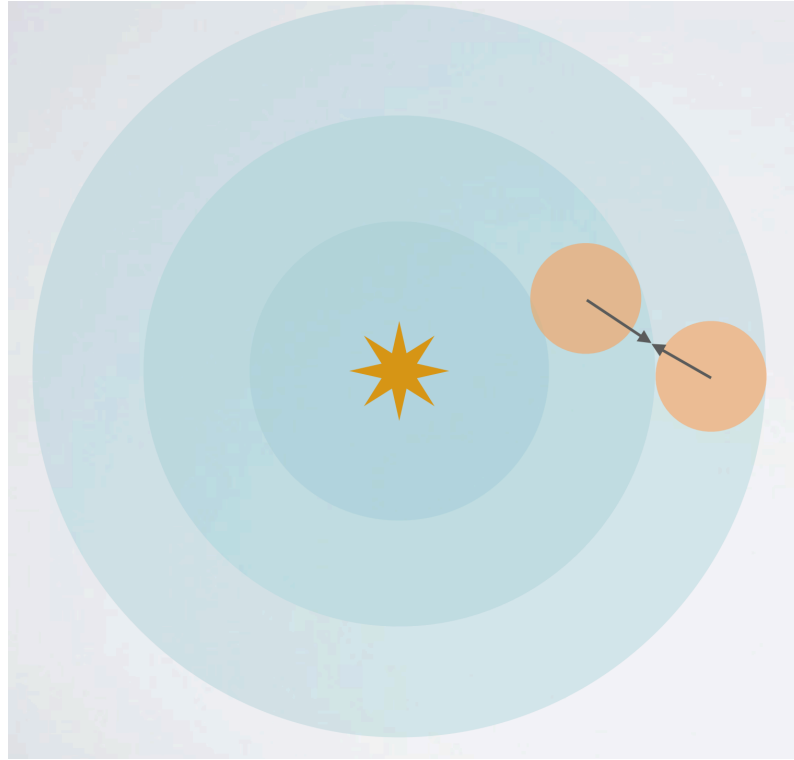
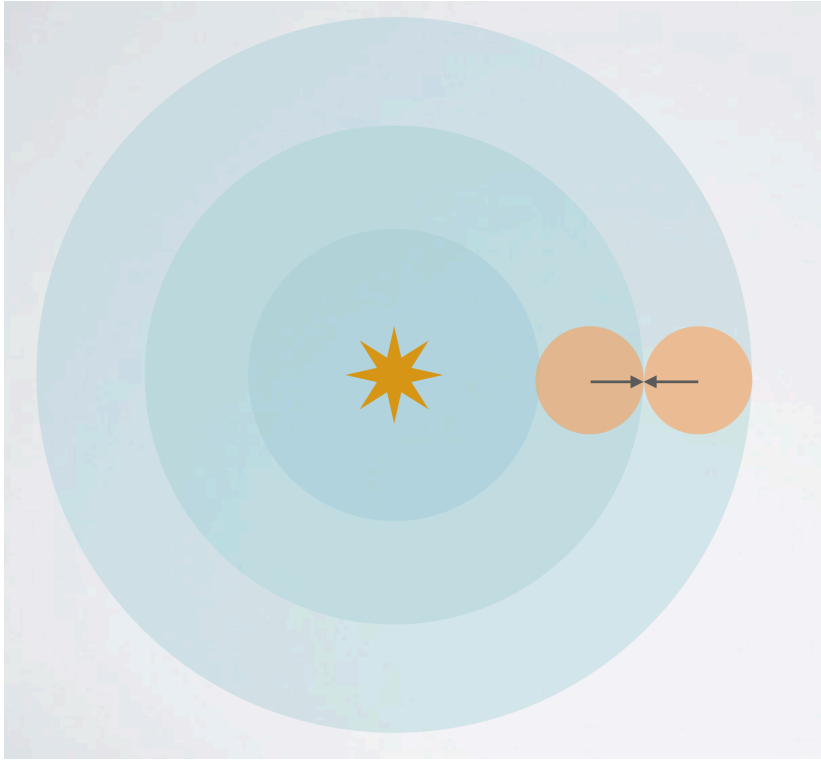
Gas falls toward star

Wind launching

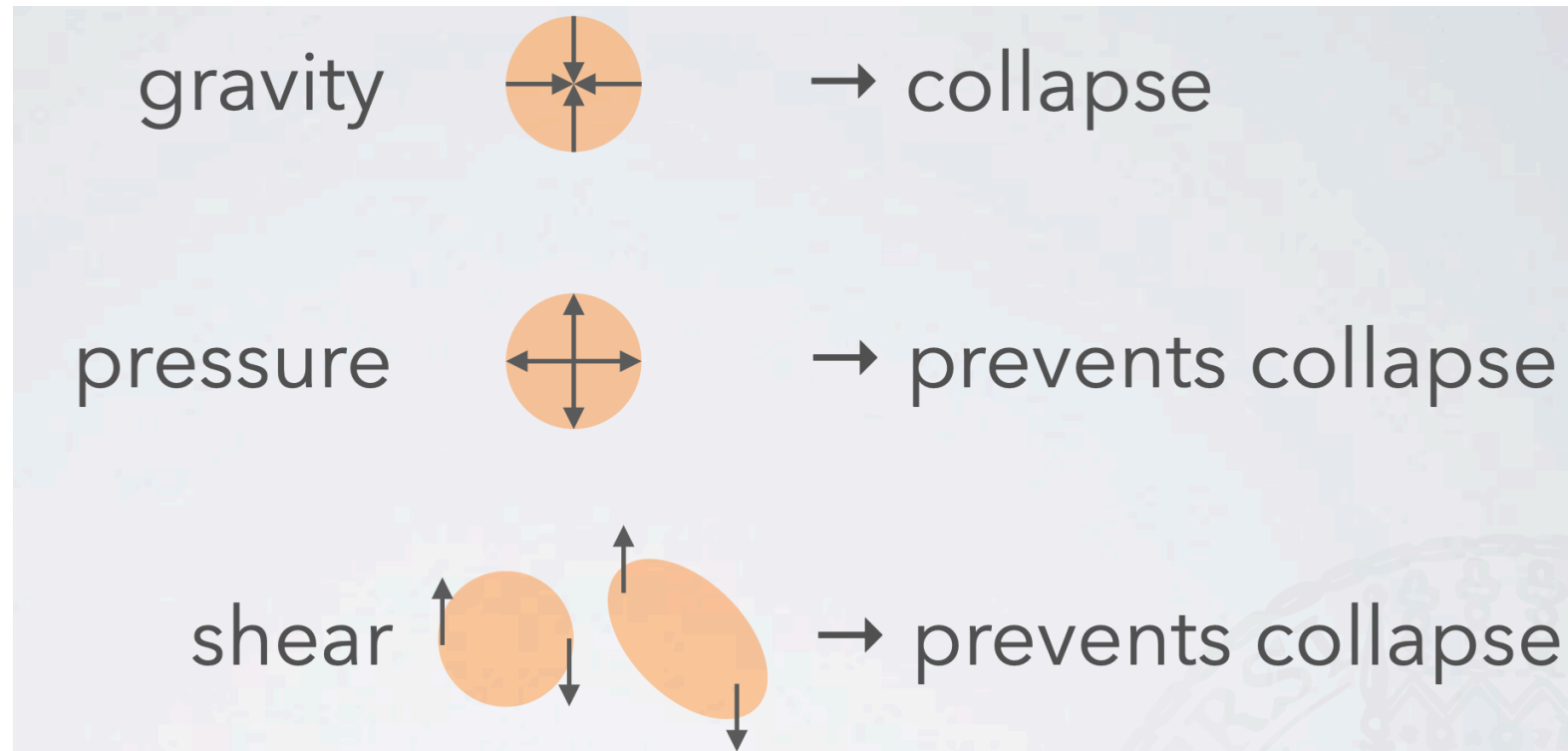


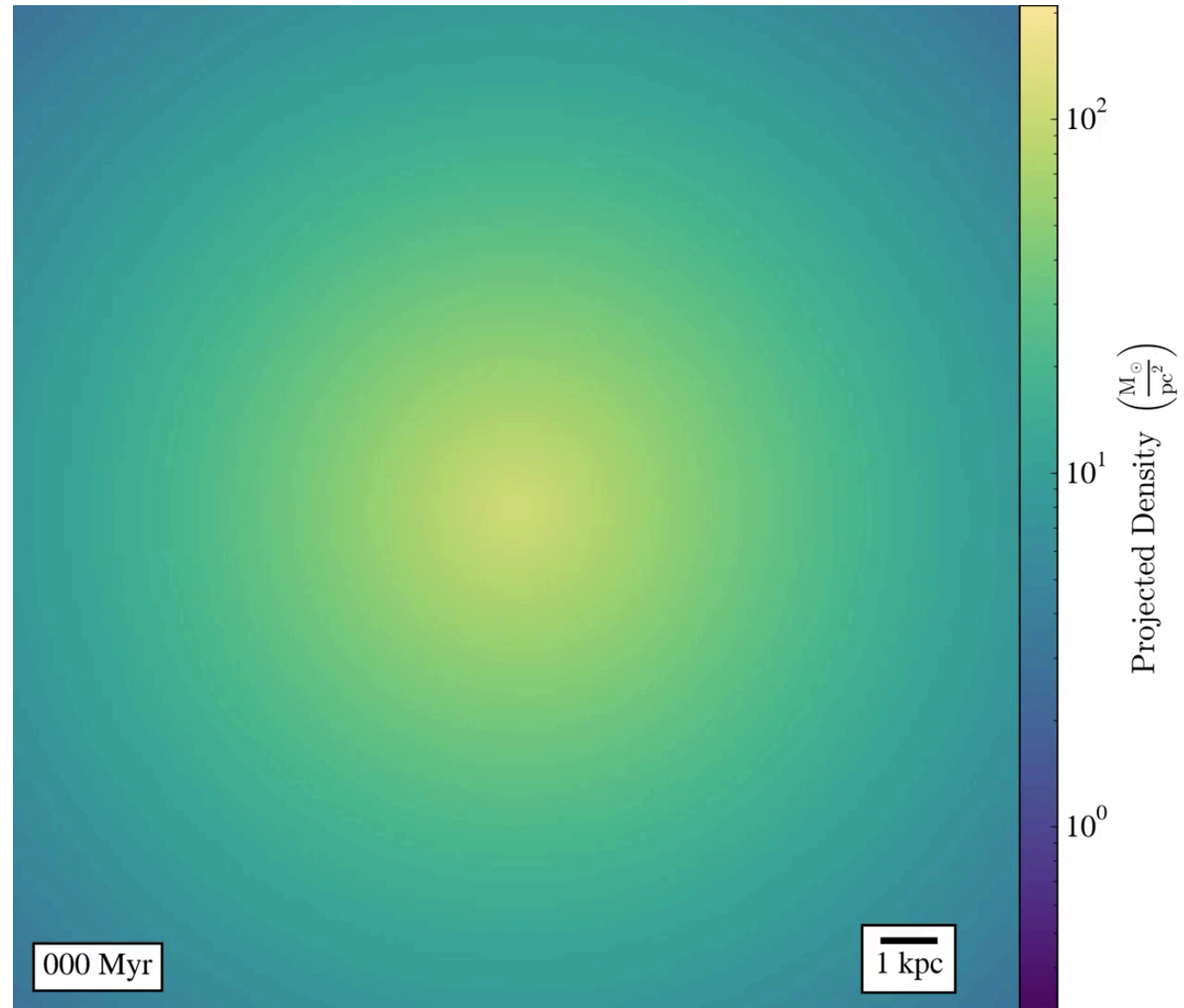


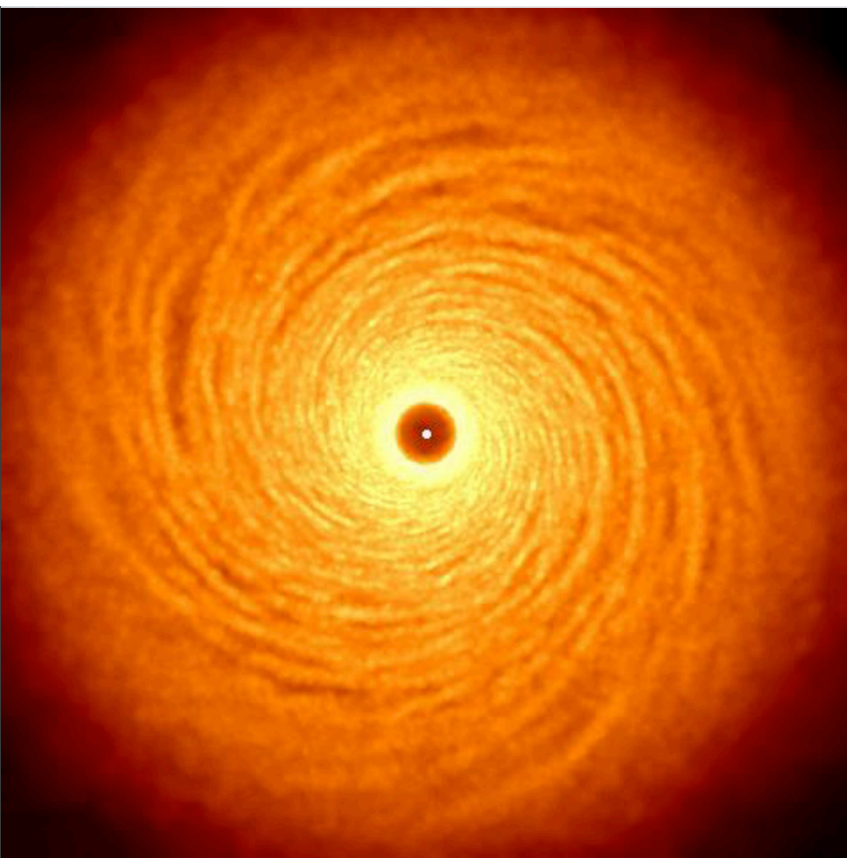
Self gravity



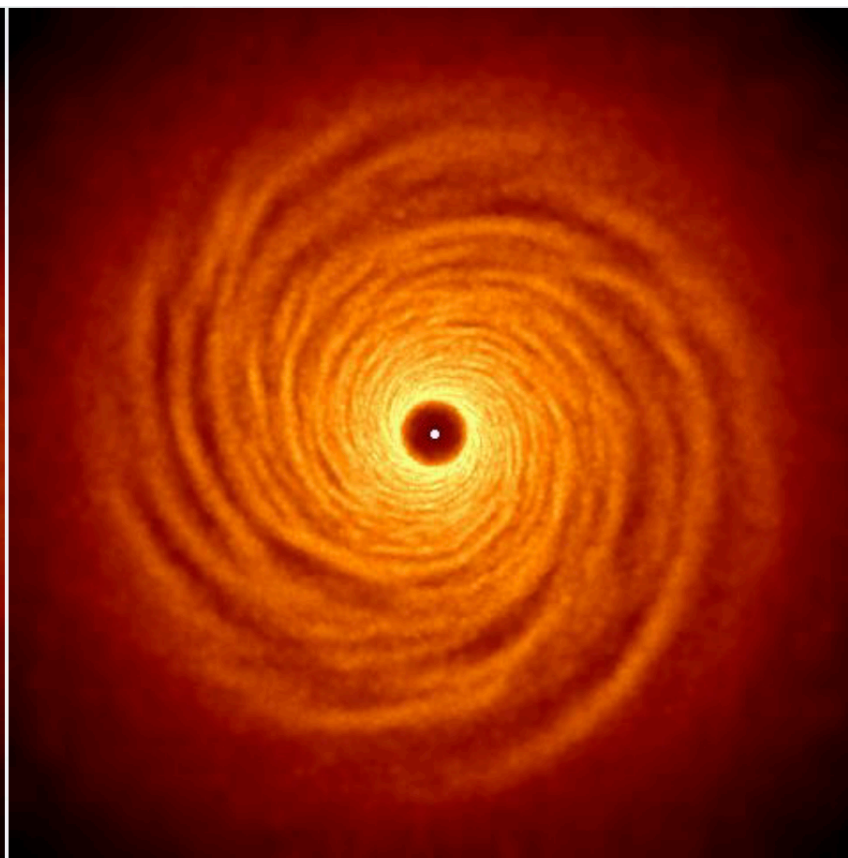
Self gravity



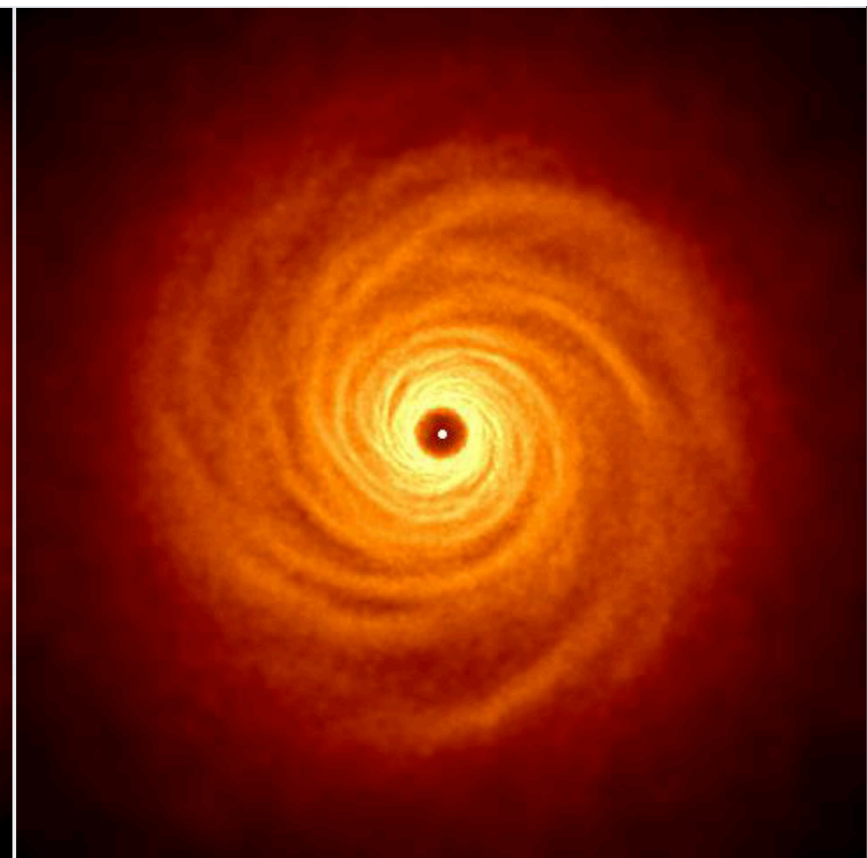




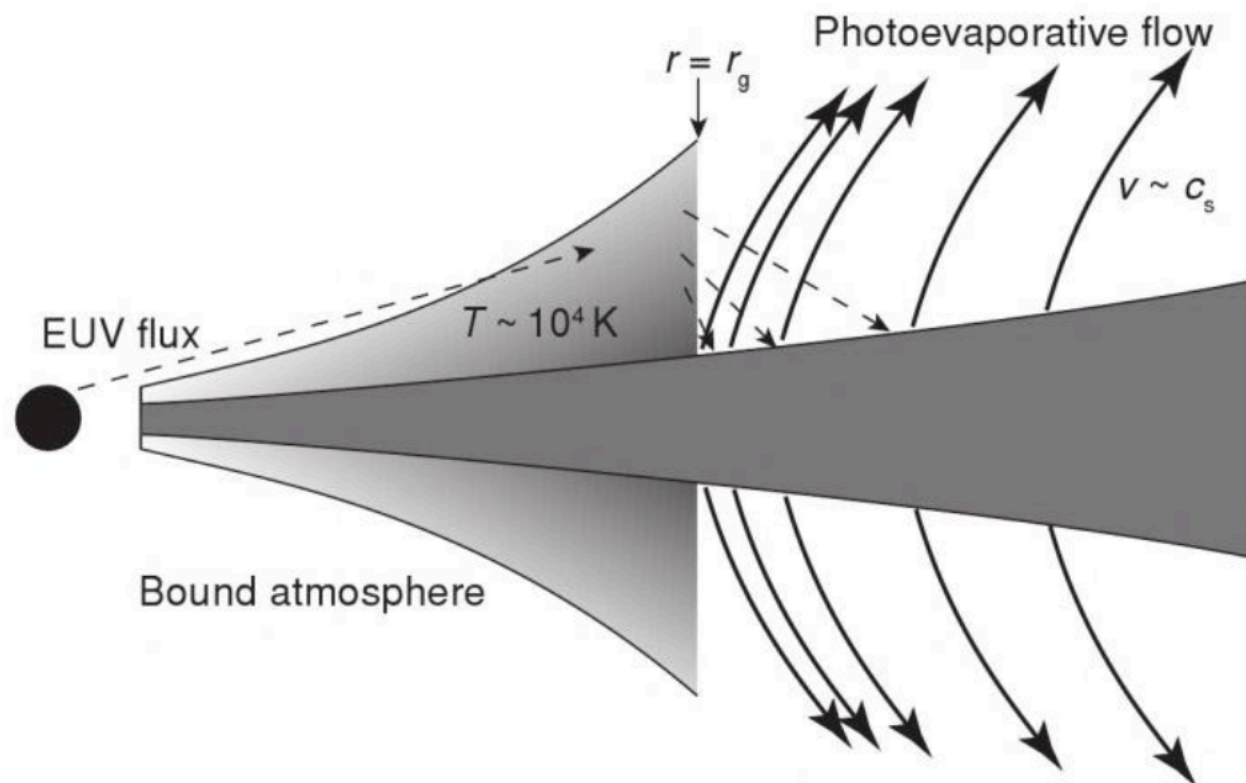
$$M_{\text{disk}}/M_{\star} = 0.05$$



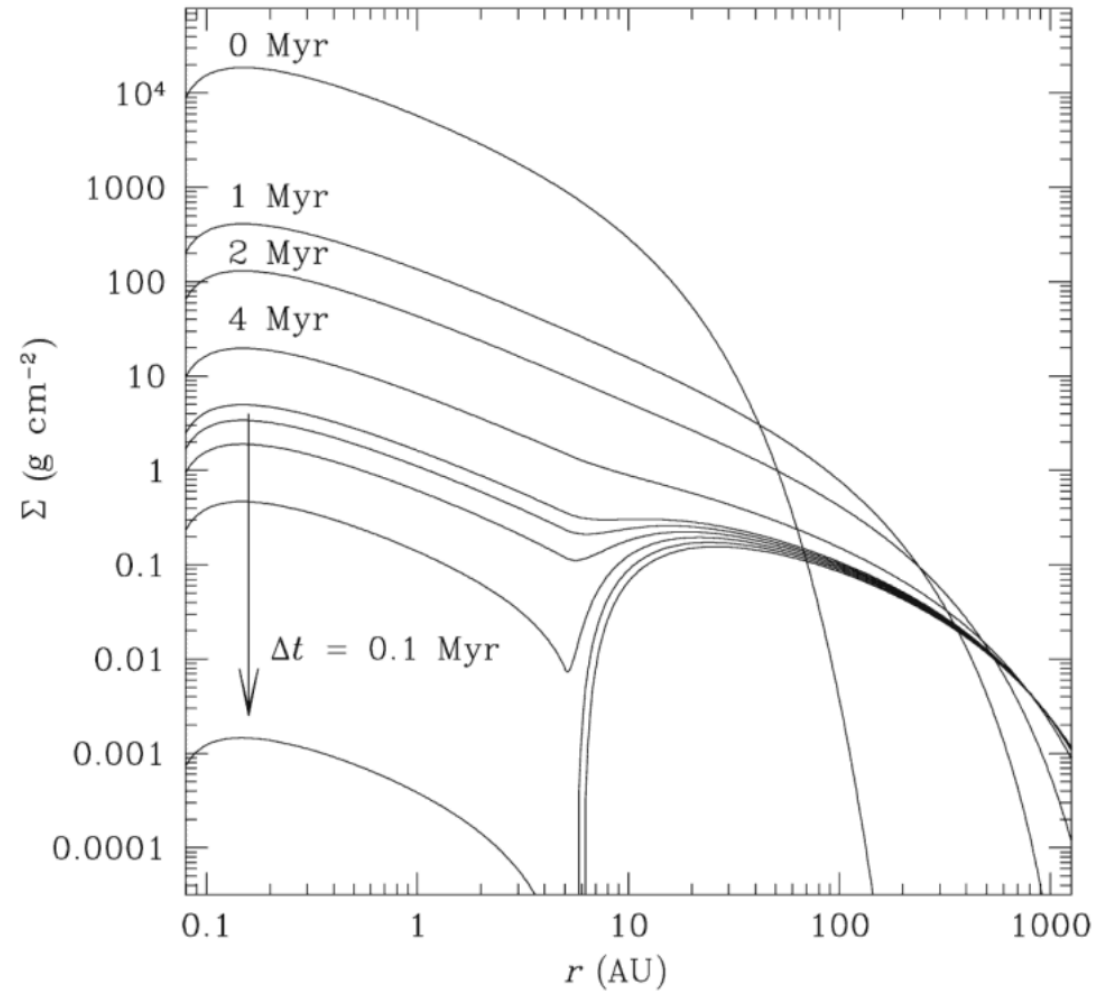
$$M_{\text{disk}}/M_{\star} = 0.1$$

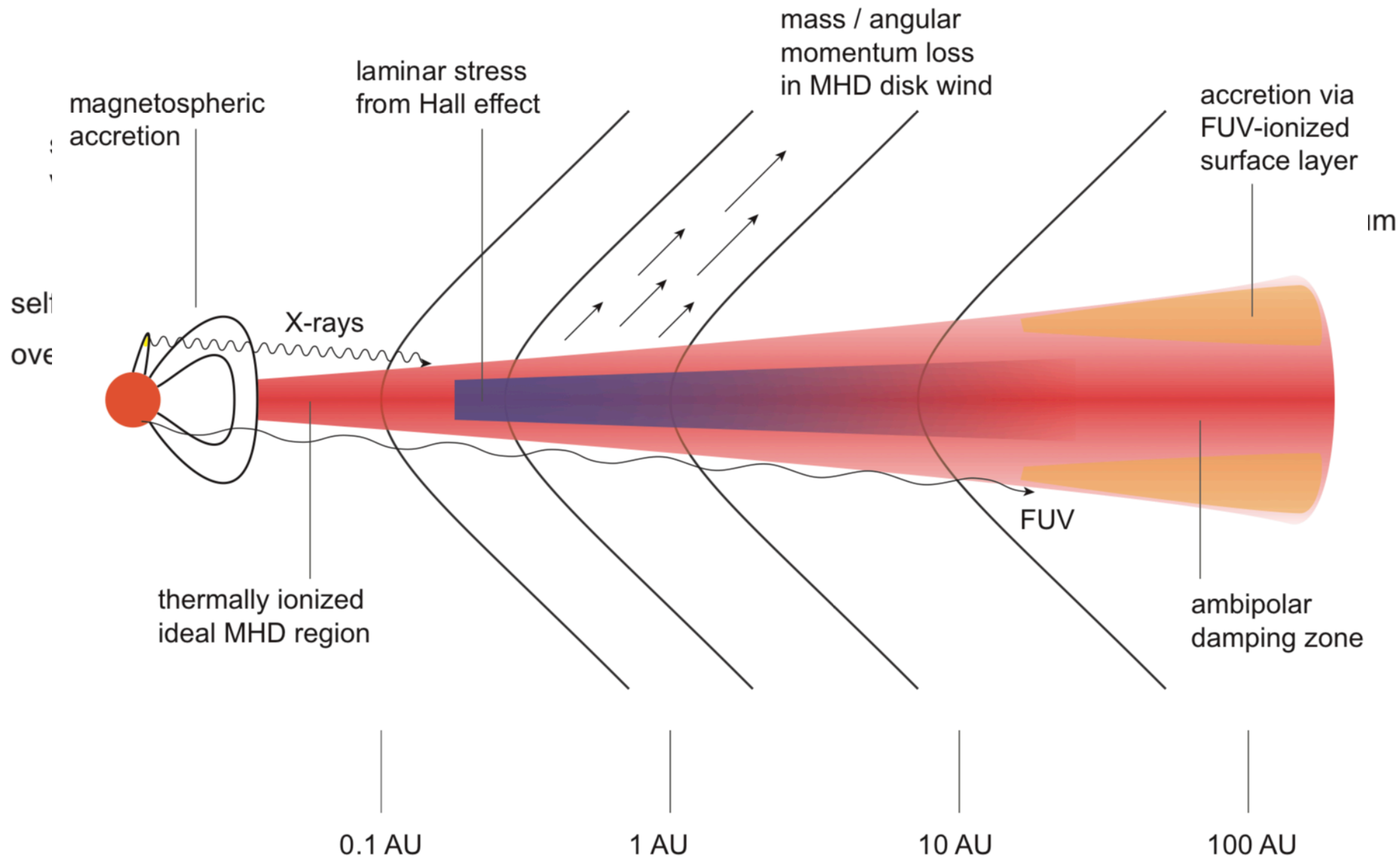


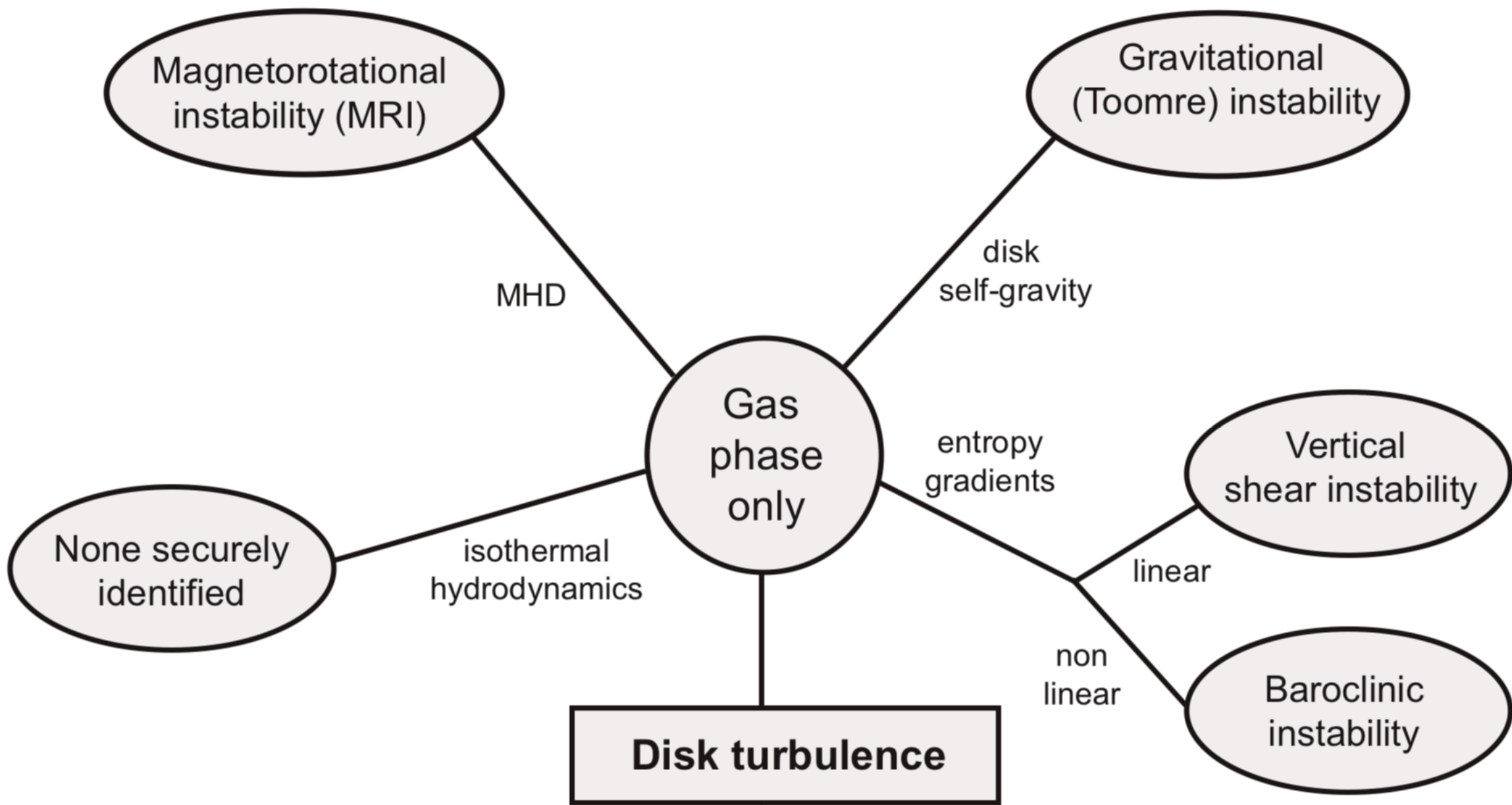
$$M_{\text{disk}}/M_{\star} = 0.25$$



Accretion and Photoevaporation







CONVECTIVE OVERSTABILITY IN ACCRETION DISKS: THREE-DIMENSIONAL LINEAR ANALYSIS AND NONLINEAR SATURATION

VLADIMIR LYRA^{1,2,3}

¹ Jet Propulsion Laboratory, California Institute of Technology, 4800 Oak Grove Drive, Pasadena, CA 91109, USA; wlyra@caltech.edu

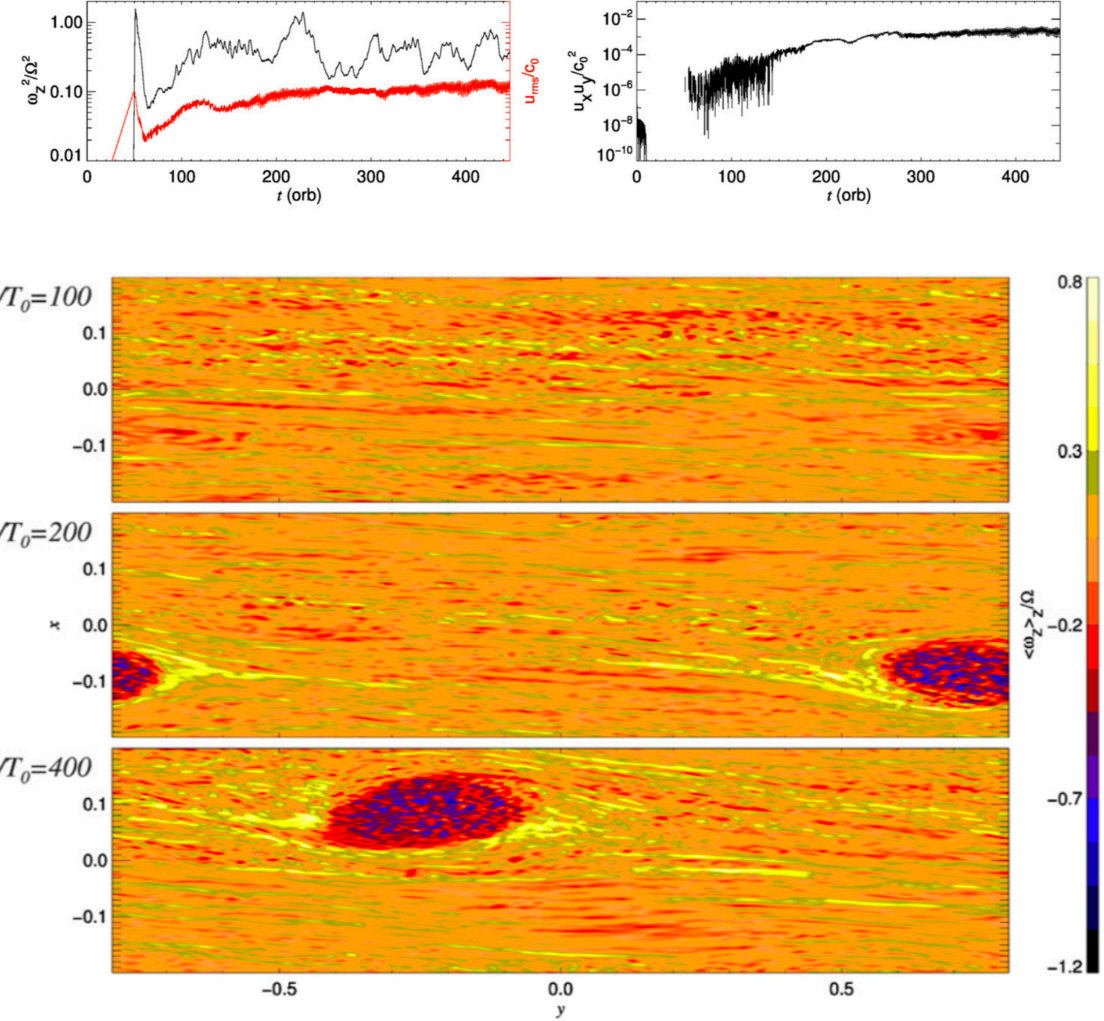
² Department of Geology and Planetary Sciences, California Institute of Technology, 1200 E. California Avenue, Pasadena, CA 91125, USA
 Received 2014 April 21; accepted 2014 May 13; published 2014 June 17

ABSTRACT

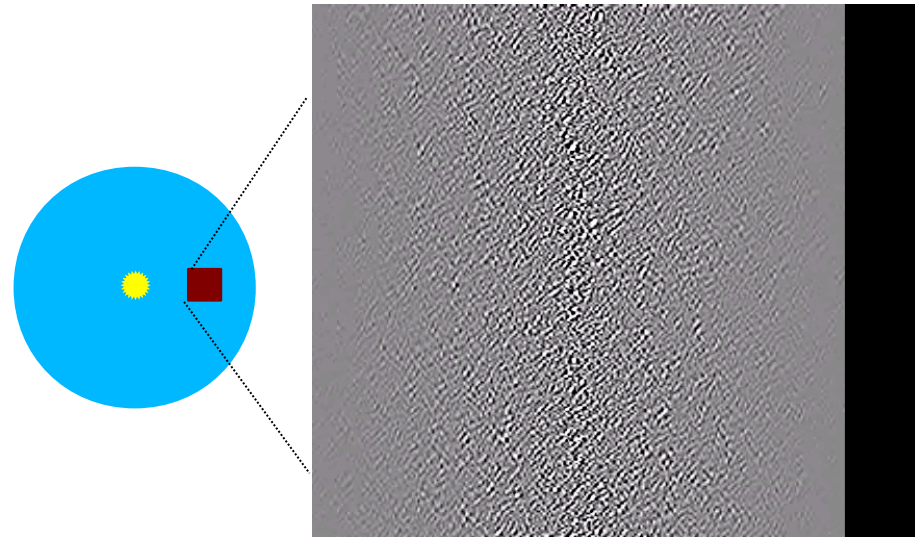
Recently, Klahr & Hubbard claimed that a hydrodynamical linear overstability exists in protoplanetary disks, powered by buoyancy in the presence of thermal relaxation. We analyze this claim, confirming it through rigorous compressible linear analysis. We model the system numerically, reproducing the linear growth rate for all cases studied. We also study the saturated properties of the overstability in the shearing box, finding that the saturated state produces finite amplitude fluctuations strong enough to trigger the subcritical baroclinic instability (SBI). Saturation leads to a fast burst of enstrophy in the box, and a large-scale vortex develops in the course of the next ≈ 100 orbits. The amount of angular momentum transport achieved is of the order of $\alpha \approx 10^{-3}$, as in compressible SBI models. For the first time, a self-sustained three-dimensional vortex is produced from linear amplitude perturbation of a quiescent base state.

Key words: hydrodynamics – instabilities – methods: analytical – methods: numerical – planets and satellites: formation – protoplanetary disks

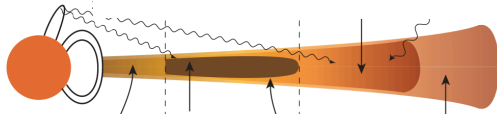
Online-only material: color figures



Convective Overstability

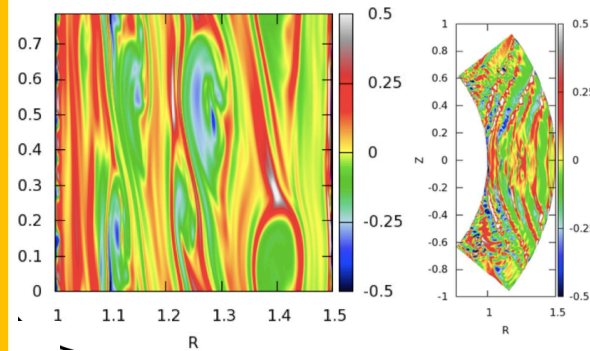


Lyra & Klahr (2011)



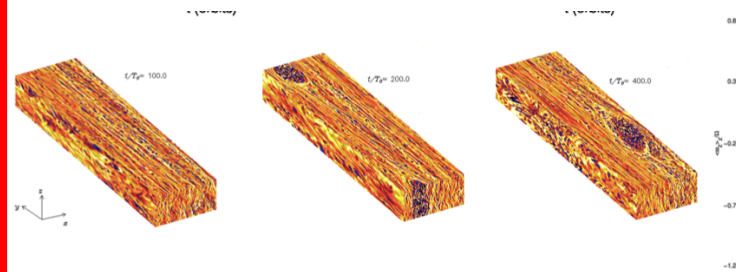
Hydrodynamical Instabilities

Vertical Shear Instability



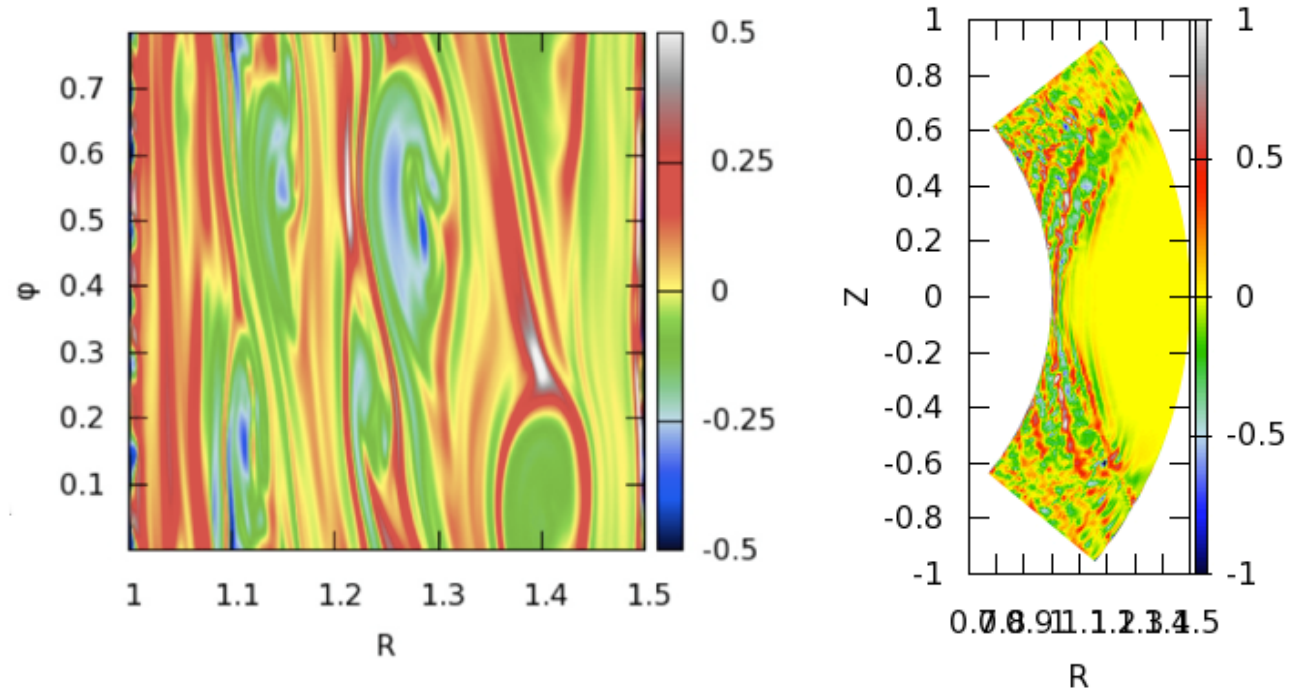
Nelson et al. 2013, Lin & Youdin 2015, Umrhan et al. 2016

Convective Overstability



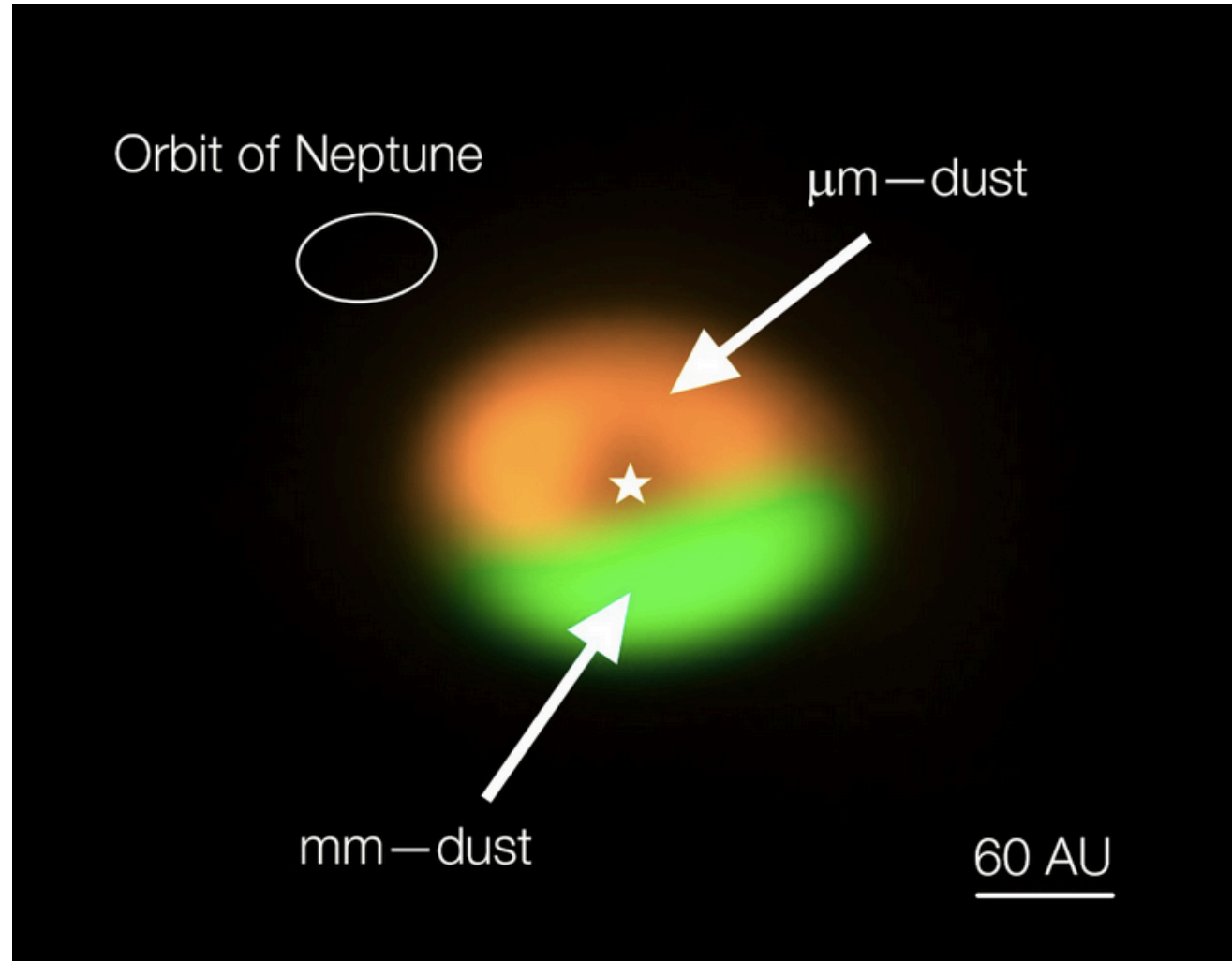
Klahr 2003, Lesur & Papaloizou 2010, Lyra & Klahr 2011, Lyra 2014

Vertical shear instability



Nelson et al. (2013)

Oph IRS 48



eso1325 — Science Release

ALMA Discovers Comet Factory

New observations of a “dust trap” around a young star solve long-standing planet formation mystery

6 June 2013



A Major Asymmetric Dust Trap in a Transition Disk

Nienke van der Marel,^{1*} Ewine F. van Dishoeck,^{1,2} Simon Bruderer,² Til Birnstiel,³ Paola Pinilla,⁴ Cornelis P. Dullemond,⁴ Tim A. van Kempen,^{1,5} Markus Schmalz,¹ Joanna M. Brown,³ Gregory J. Herczeg,⁶ Geoffrey S. Mathews,¹ Vincent Geers⁷

The statistics of discovered exoplanets suggest that planets form efficiently. However, there are fundamental unsolved problems, such as excessive inward drift of particles in protoplanetary disks during planet formation. Recent theories invoke dust traps to overcome this problem. We report the detection of a dust trap in the disk around the star Oph IRS 48 using observations from the Atacama Large Millimeter/submillimeter Array (ALMA). The 0.44-millimeter-wavelength continuum map shows high-contrast crescent-shaped emission on one side of the star, originating from millimeter-sized grains, whereas both the mid-infrared image (micrometer-sized dust) and the gas traced by the carbon monoxide 6-5 rotational line suggest rings centered on the star. The difference in distribution of big grains versus small grains/gas can be modeled with a vortex-shaped dust trap triggered by a companion.

Although the ubiquity of planets is confirmed almost daily by detections of new exoplanets (1), the exact formation mechanism of planetary systems in disks of gas and dust around young stars remains a long-standing problem in astrophysics (2). In

sciencemag.org SCIENCE VOL 340 7 JUNE 2013

1199

PERSPECTIVES

van der Marel et al. 2013

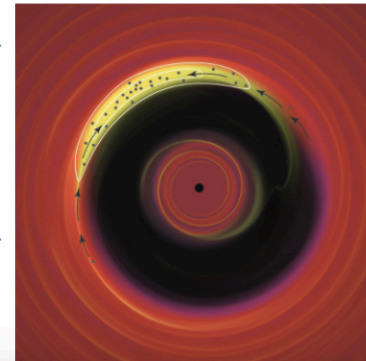
ASTRONOMY

A Trap for Planet Formation

Philip J. Armitage^{1,2}

The raw material for forming planets is micrometer to millimeter-sized particles of dust that orbit along with gas in protoplanetary disks around young low-mass stars. These disks are known to be common and to persist for several million years (1). The Kepler mission (2) showed that mature planetary systems are also common. What is not known, however, is the full sequence of steps that allows the dust within protoplanetary disks to grow into planets. On page 1199 of this issue, van der Marel *et al.* (3) report observations from the Atacama Large Millimeter/submillimeter Array (ALMA) that hint at how the most problematic step may be surmounted—millimeter-sized par-

The detection of a pocket of trapped particles may provide a hint to understanding the mechanism of planet formation.

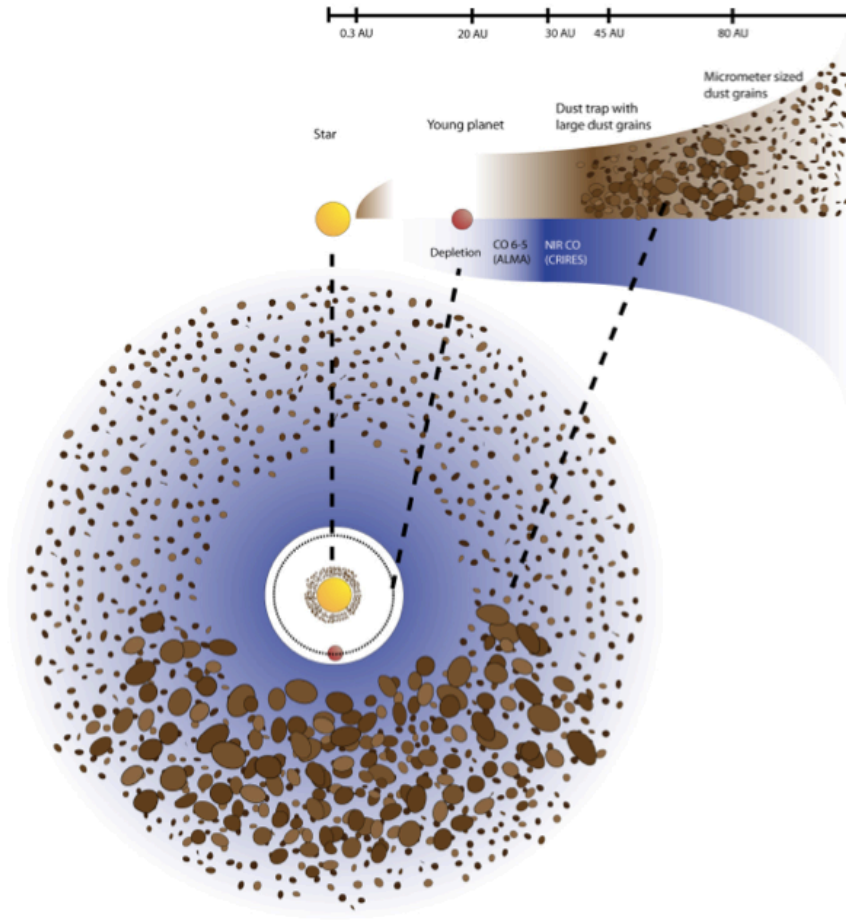


From dust to planet. Illustration of the proposed mechanism that creates a dust trap in the disk of IRS 48. A massive planet (plus symbol) creates an annular gap in the gas disk, whose surface density is shown as a color map. A high-pressure vortex (contours) forms at the gap edge, collecting and trapping millimeter-sized dust particles that would otherwise spiral rapidly inward through the disk.

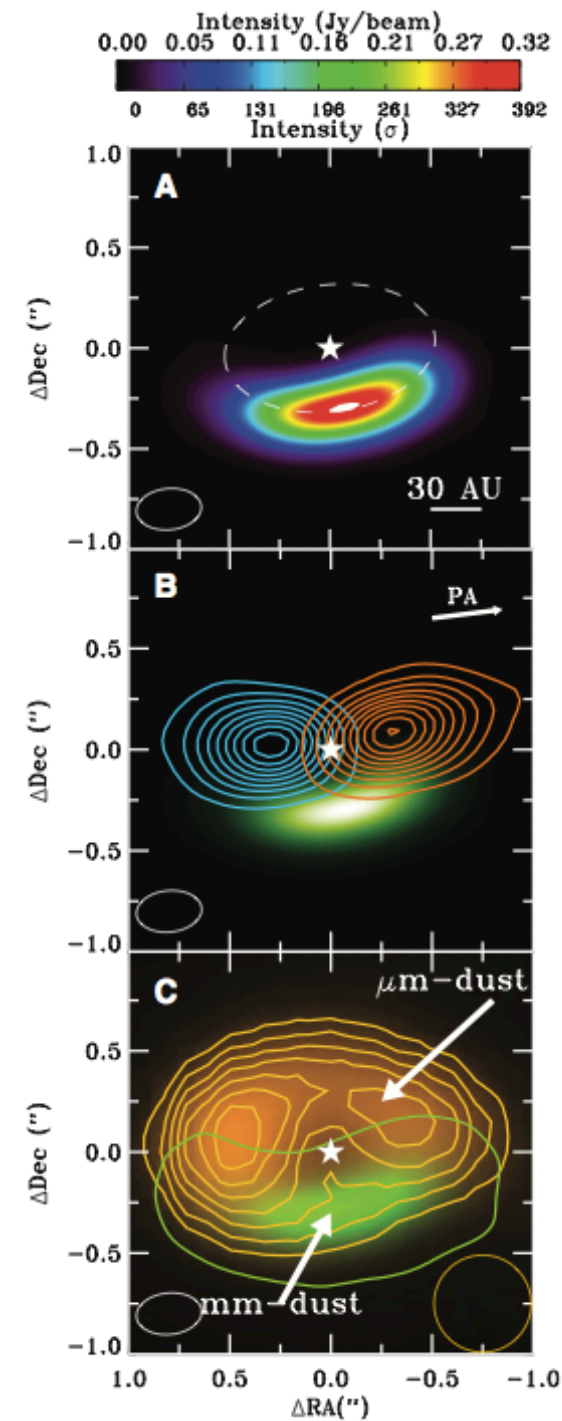
metric distribution. The emission from smaller dust particles, measured separately at infrared wavelengths, is also distributed uniformly around the orbit (11). These observations are consistent with theoretical expectations for a dust trap, in which a modest peak in gas pressure is able to strongly concentrate the millimeter-sized solid particles that

sciencemag.org on June 19, 2013

The Oph IRS 48 “dust trap”



van der Marel et al. (2013)

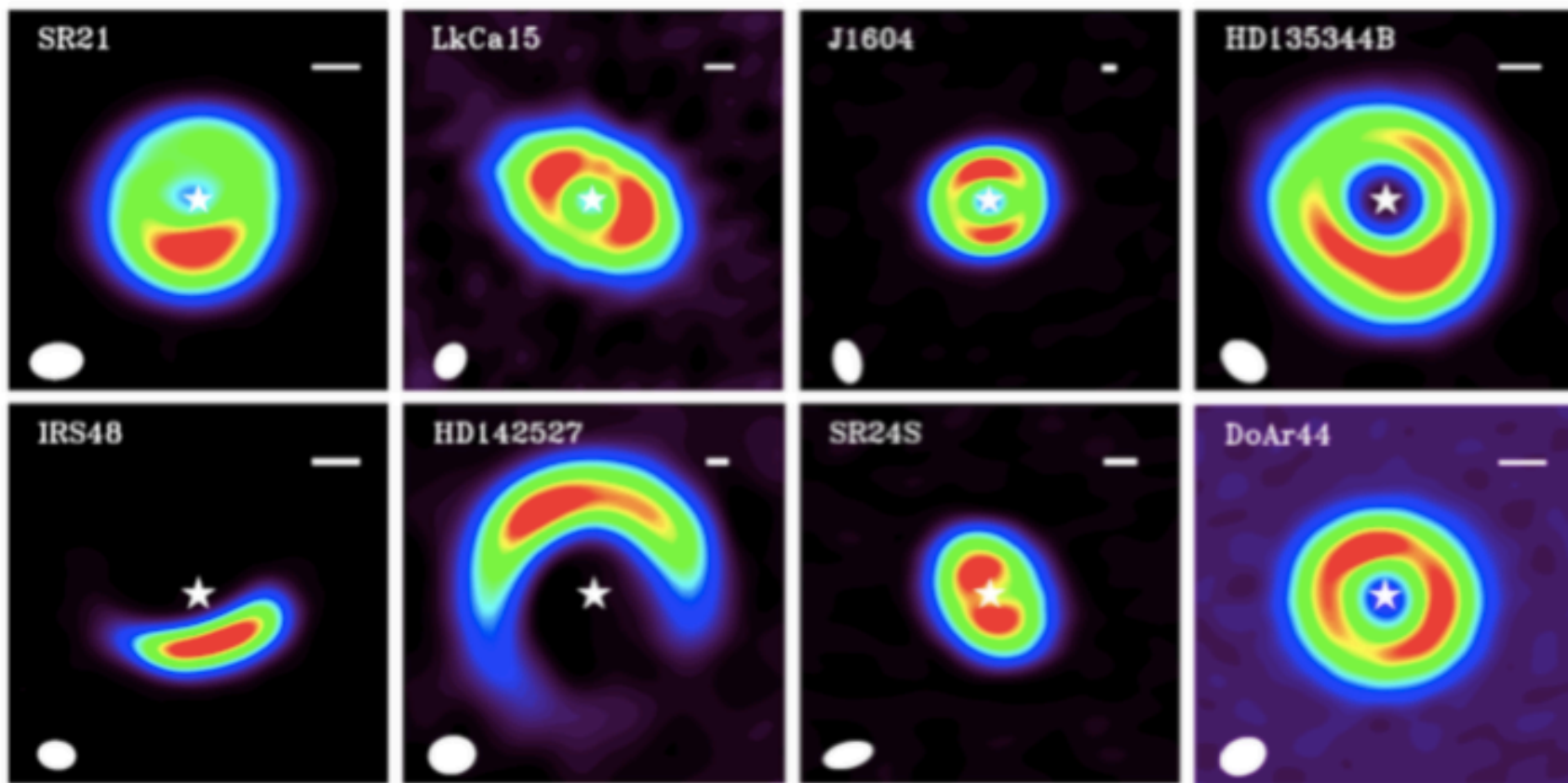


asymmetric
mm dust
at 63 AU

Gas detection:
Keplerian rotation

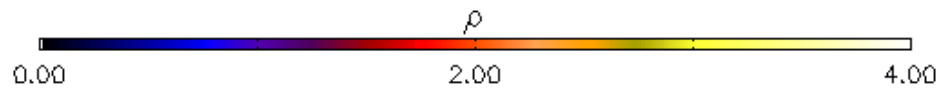
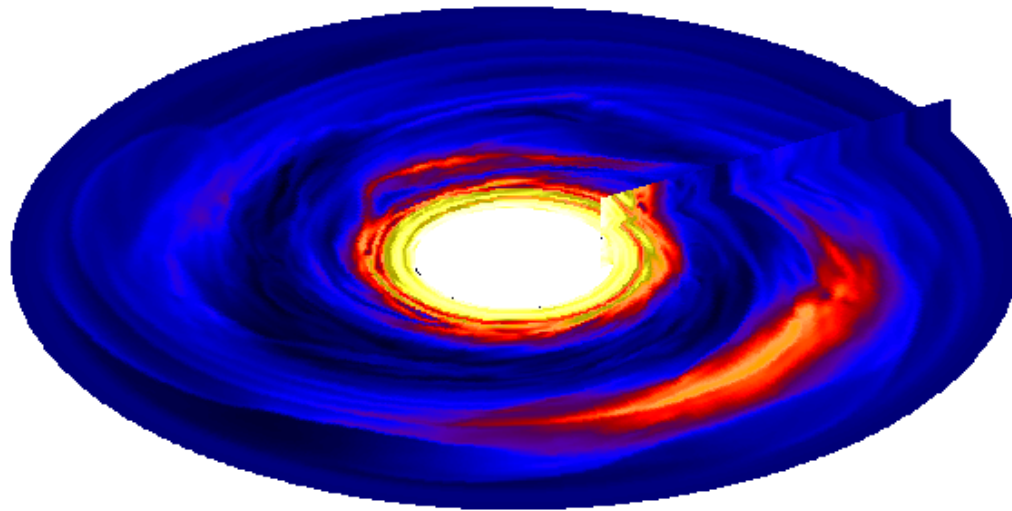
Micron-sized
dust follows gas

“Asymmetries” everywhere



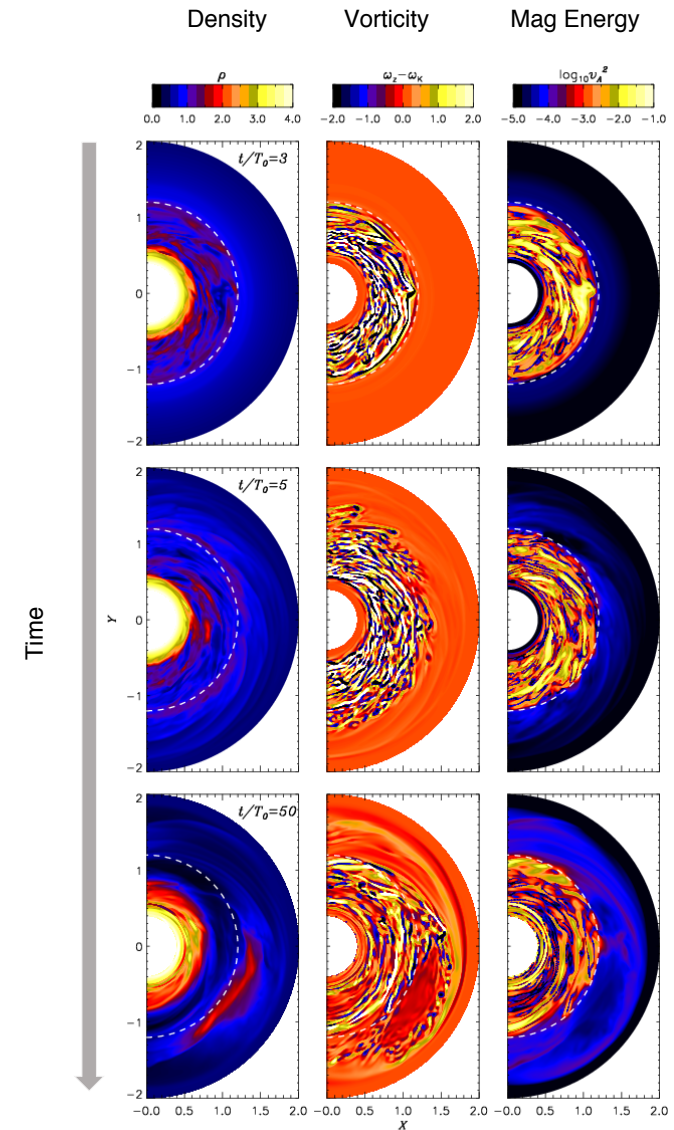
Active/dead zone boundary

$t = 22.28 \tau_D$

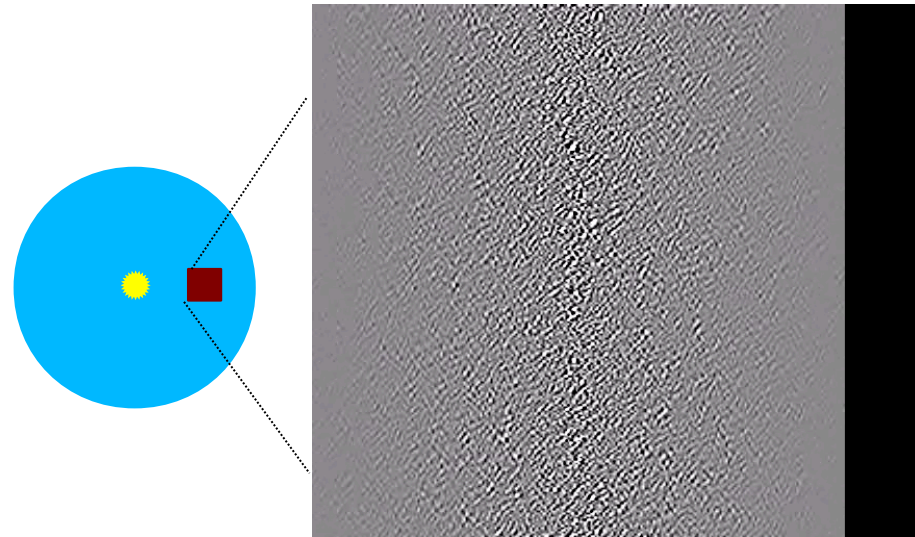


Magnetized inner disk + resistive outer disk

Lyra & Mac Low (2012)

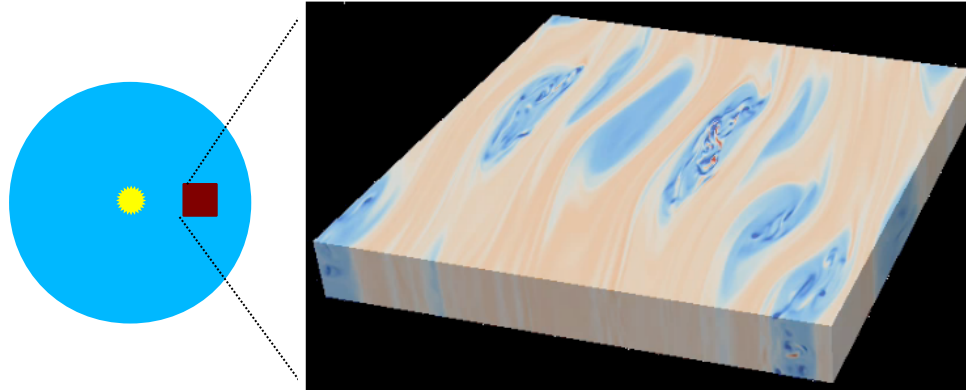


Convective Overstability



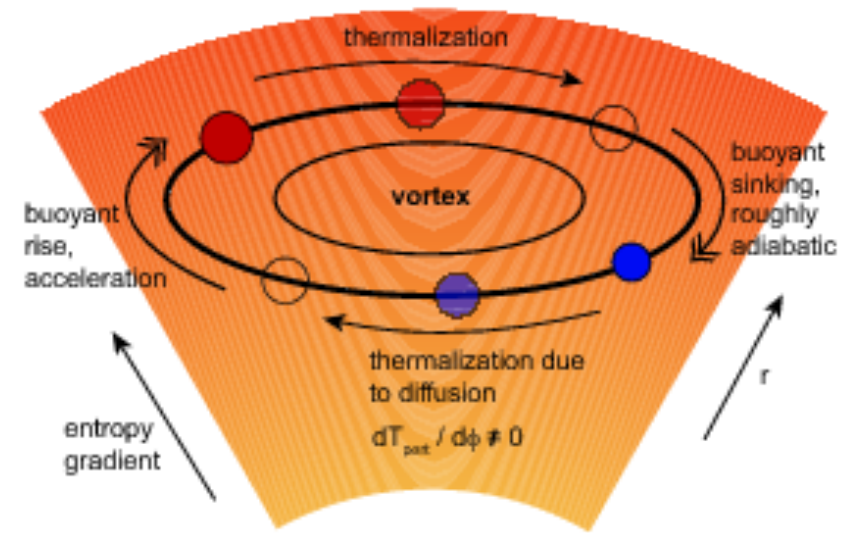
Lyra & Klahr (2011)

Convection



Lesur & Papaloizou (2010)

Sketch of Convection



Armitage (2010)



Convective Overstability

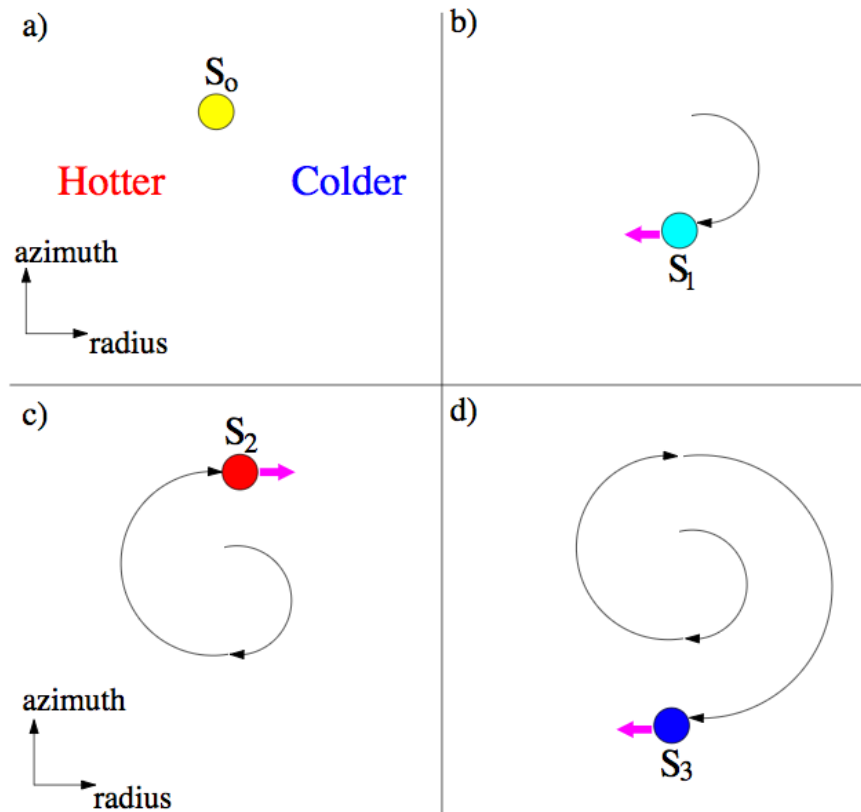
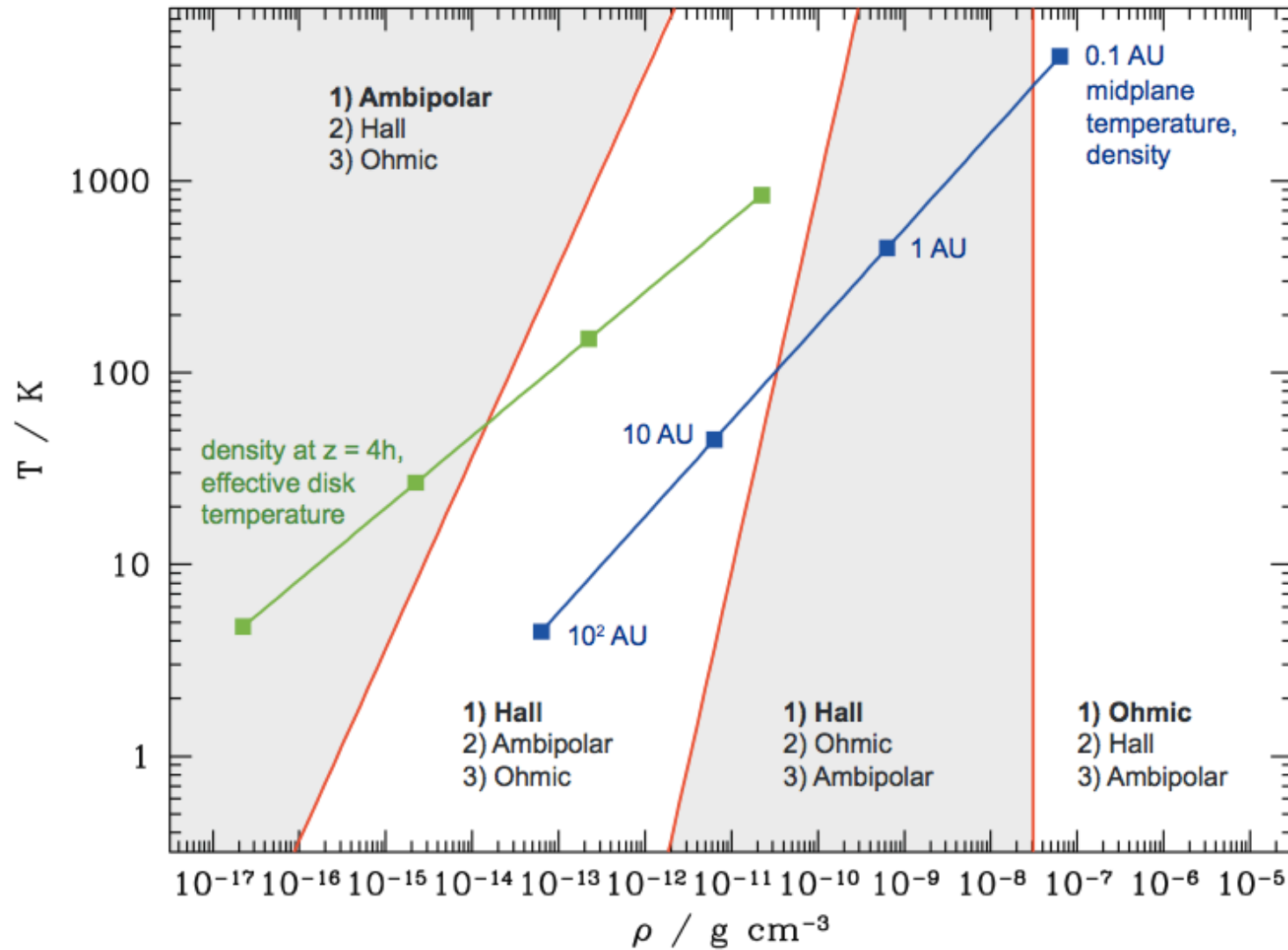
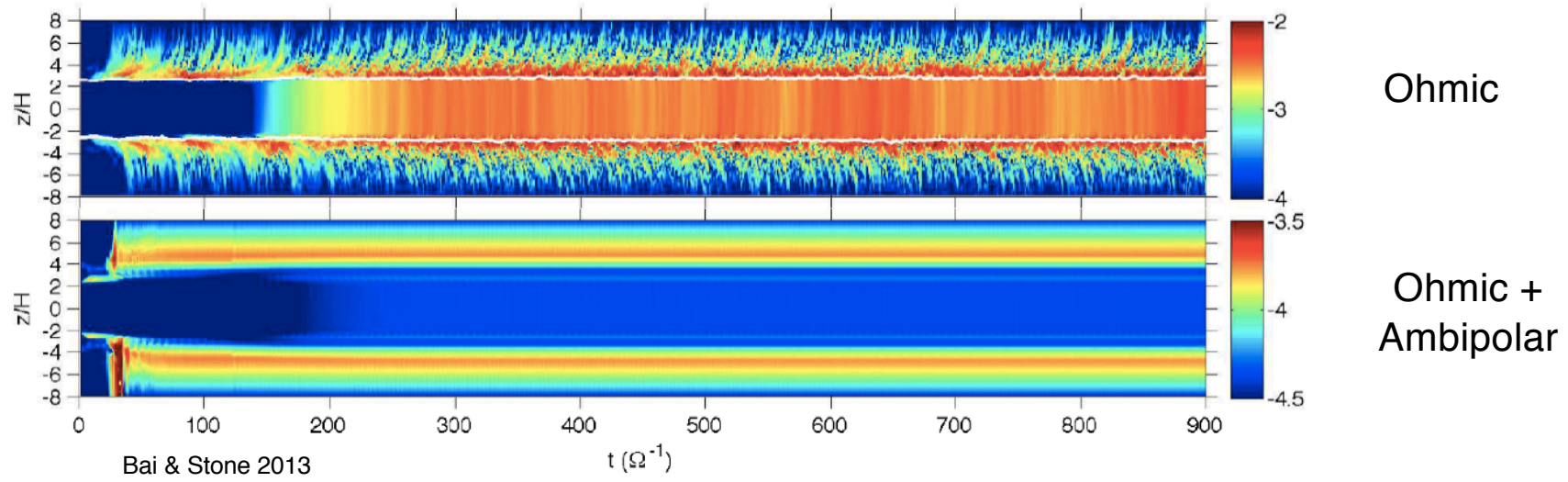


Figure 2. Four panels indicating the convective overstability mechanism. In panel (a) a fluid blob is embedded in a radial entropy gradient. In panel (b) it undergoes half an epicycle and returns to its original radius with a smaller entropy than when it began $S_1 < S_0$. It hence feels a buoyancy acceleration inwards and the epicycle is amplified. The process occurs in reverse once the epicycle is complete, shown in panel (c), where now $S_2 > S_0$. The oscillations hence grow larger and larger.

Non-ideal MHD: Ohmic, Hall, Ambipolar terms



Ambipolar diffusion



Ambipolar diffusion

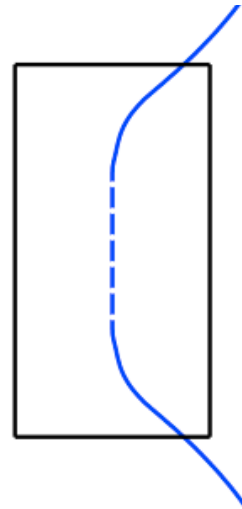
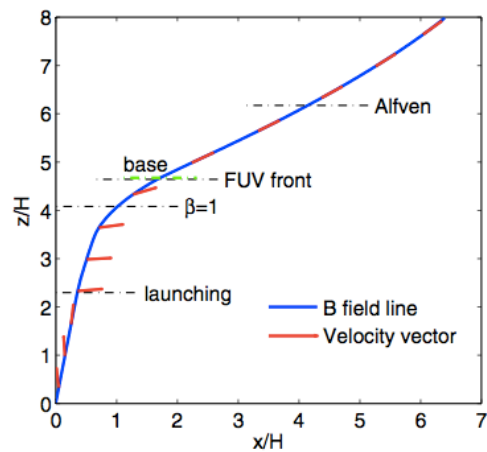
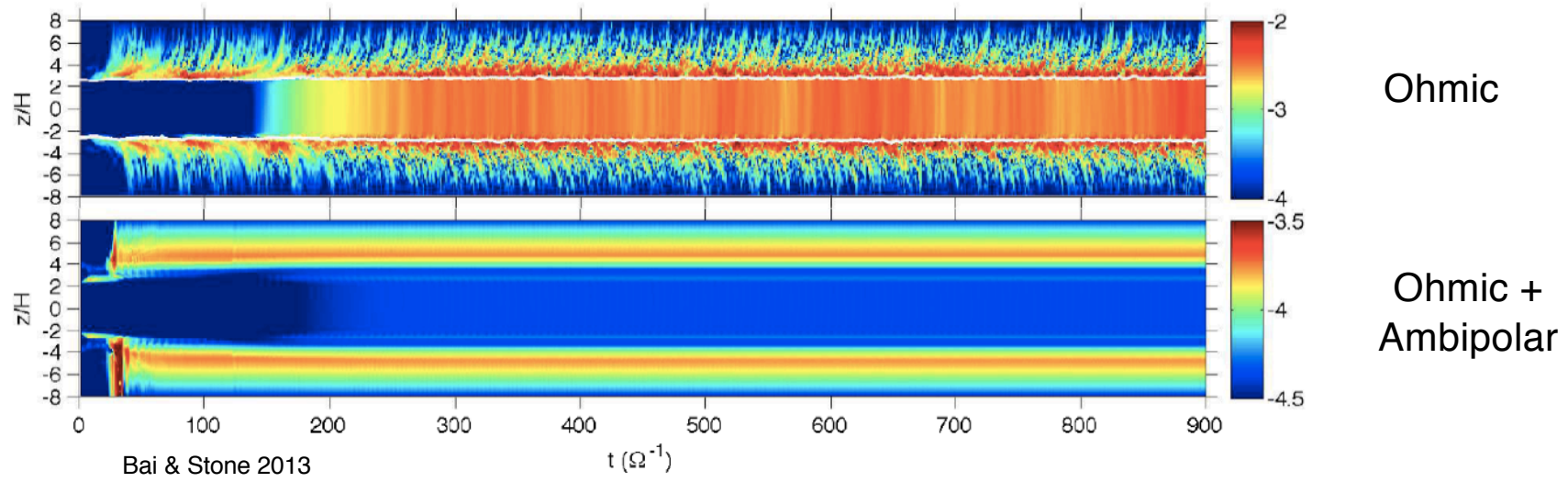


Figure 6. Poloidal field line geometry in our fiducial run OA-b5 (blue solid line). Overplotted are the unit vectors of the poloidal gas velocity (red arrows). The location of the wind launching point, the plasma $\beta = 1$ point, the FUV ionization front, and the Alfvén point are indicated (black dash-dotted). Also marked is the location at the base of the wind (green dashed).

Ambipolar diffusion

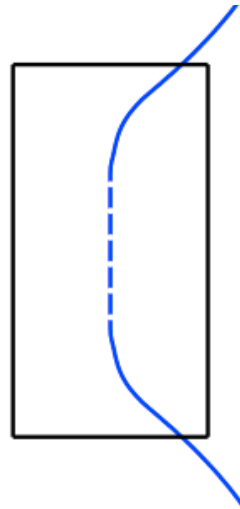
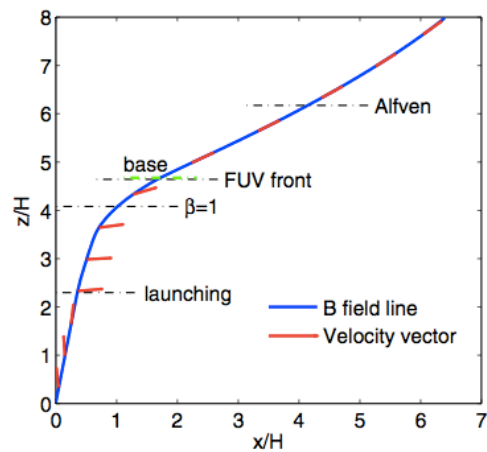
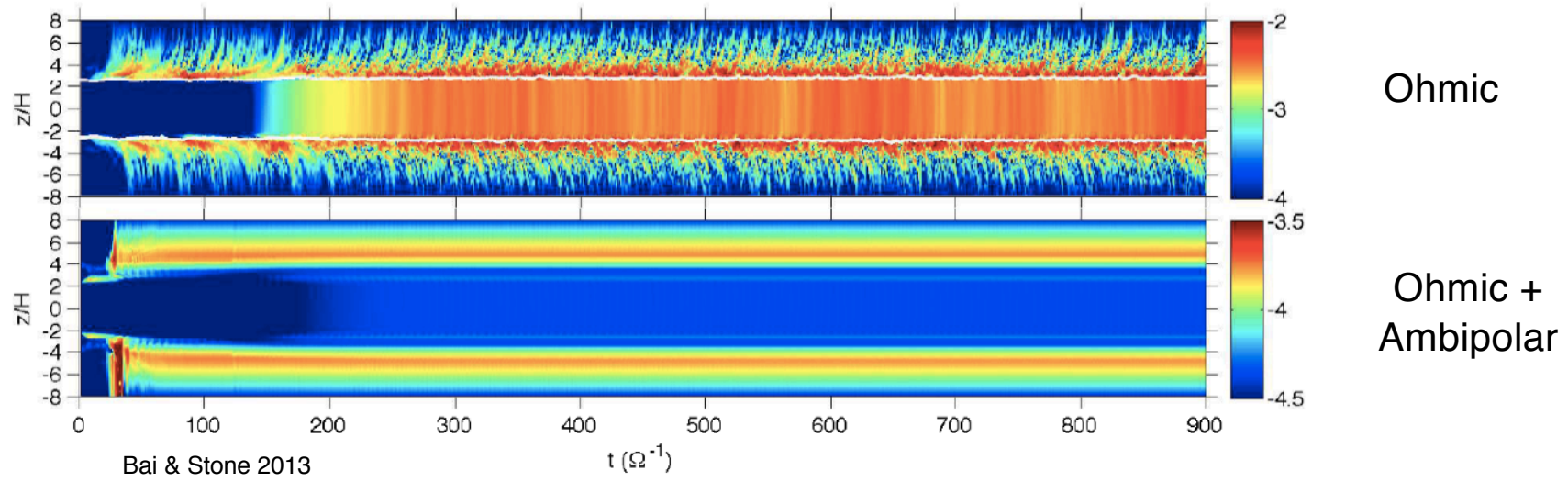
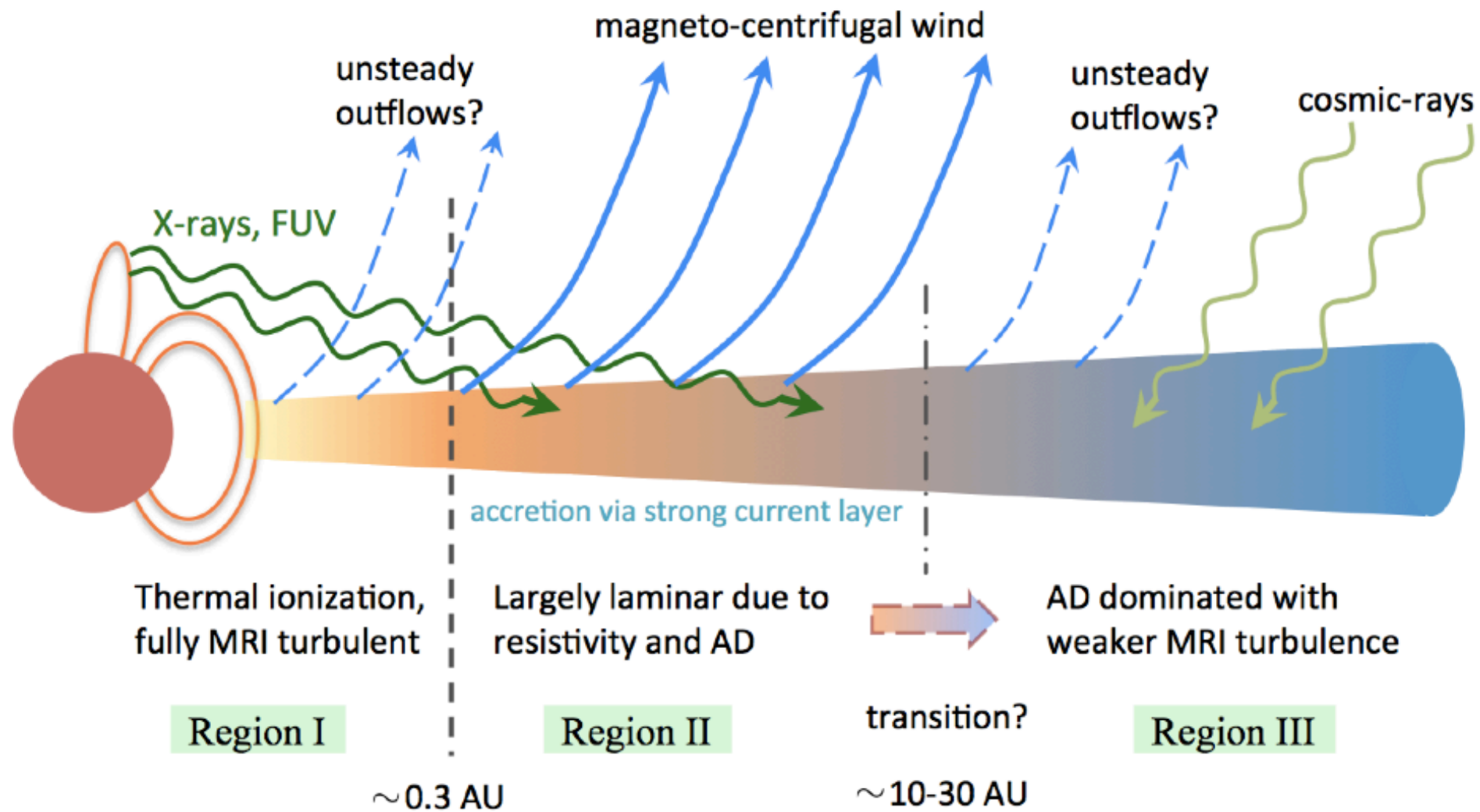
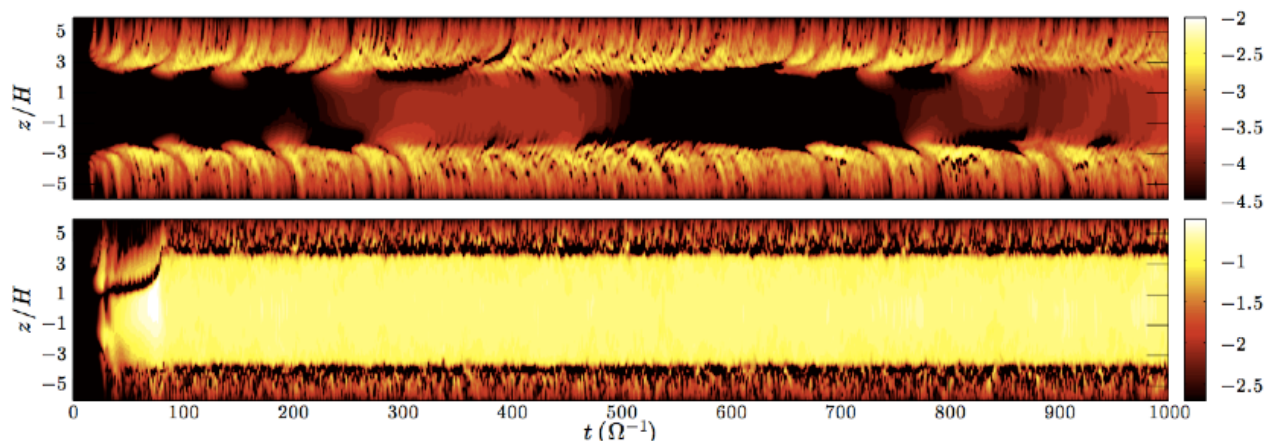
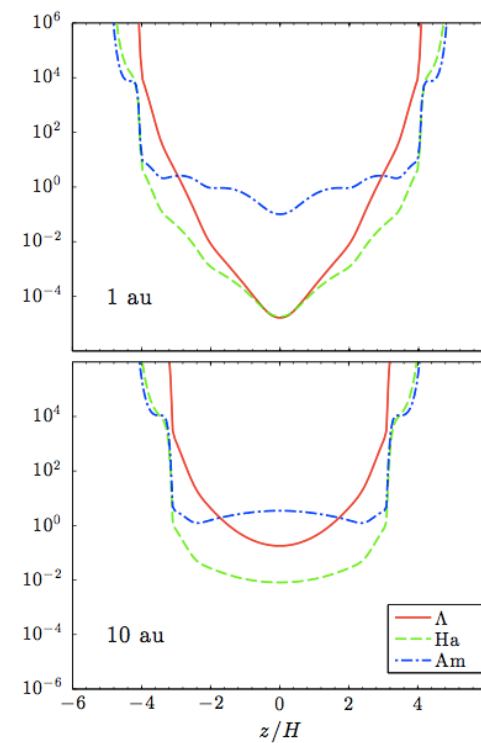


Figure 6. Poloidal field line geometry in our fiducial run OA-b5 (blue solid line). Overplotted are the unit vectors of the poloidal gas velocity (red arrows). The location of the wind launching point, the plasma $\beta = 1$ point, the FUV ionization front, and the Alfvén point are indicated (black dash-dotted). Also marked is the location at the base of the wind (green dashed).



Hall term

Large-scale azimuthal field generated. Couples to
radial field fluctuations to generate large stress.
The flow stays laminar



Ohmic

Ohmic + Hall

Fig. 6. Space-time diagram of the logarithm of the horizontally averaged Maxwell stress, $\log\langle -B_x B_y \rangle$, in the Ohmic (1-O-5; top) and Ohmic-Hall (1-OH-5; bottom) runs.

The full monty

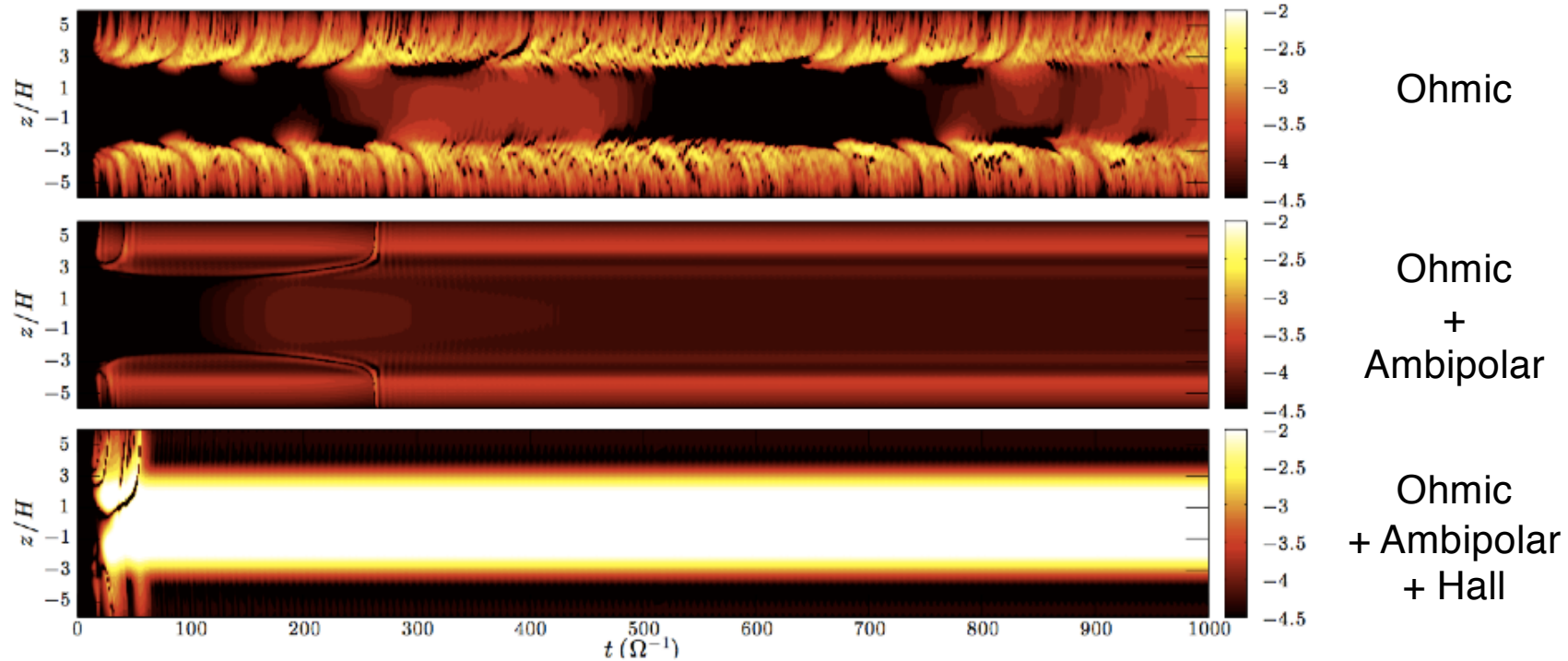


Fig. 9. Space-time evolution of the logarithm of the horizontally-averaged magnetic stress, $\log\langle M_{xy} \rangle$, in the Ohmic (1-O-5; top), Ohmic-ambipolar (1-OA-5; middle), and Ohmic-ambipolar-Hall (1-OHA-5; bottom) runs.

Ambipolar “kills” accretion.
Hall “ressurects” it.

Large scale B_ϕ couples to δB_r leading to laminar stress.
Wind is also amplified.

